CHAPTER 4

Macroparticle Models

In Chapter 2, we studied the wake fields generated by a beam in the vacuum chamber of an accelerator. In that study, we assumed that the particle distribution within the beam is rigid and that the beam motion is unperturbed by the wake fields other than the parasitic energy losses. In Chapter 3, these results were applied to study the effect of wake fields acting back upon the beam in linacs. In particular, we have considered a few one- and two-particle models in which the beam is represented simply as one or two macroparticles interacting with the vacuum chamber surroundings and, in the case of two-particle models, among themselves.

A one-particle model, in which a rigid, structureless beam interacts with its own wake fields, is the simplest model that describes the beam-environment interaction. A two-particle model offers the opportunity of looking into the instability mechanisms associated with the internal degrees of freedom in the beam distribution.

In linacs, the macroparticles are considered frozen in their relative longitudinal positions. For circular accelerators this is no longer true, because particles execute longitudinal synchrotron oscillations, and the instability analysis becomes more involved. In this chapter, a few one- and two-particle models will be developed to illustrate the various longitudinal and transverse instabilities encountered by bunched beams in circular accelerators.

The advantage of the simplified one- and two-particle models is that they provide an intuitive picture of the instability mechanisms. In fact, we find these models sufficiently useful that we are dedicating the present chapter to them. A full account of the internal beam motions will be postponed until

Chapter 6, where most of the results obtained in this chapter will be rederived systematically using the Vlasov formalism.[1]

4.1 ROBINSON INSTABILITY

The mechanism of the Robinson instability is one of the most basic instability mechanisms encountered in circular accelerators. The radio frequency (rf) accelerating cavities in a circular accelerator are tuned so that the resonant frequency ω_R of the fundamental mode[2] is very close to an integral multiple of the revolution frequency ω_0 of the beam. This necessarily means that the wake field excited by the beam in the cavities contains a major frequency component near $\omega_R \approx h\omega_0$, or equivalently, the impedance $Z_0^{\parallel}$ has a sharp peak at $\omega_R \approx h\omega_0$, where h is an integer called the *harmonic number*.

As we will soon show, the exact value of ω_R relative to $h\omega_0$ is of critical importance for the stability of the beam. Above the transition energy, the beam will be unstable if ω_R is slightly above $h\omega_0$ and stable if slightly below. This instability mechanism was first analyzed by Robinson.[3] Since then, different approaches have been developed to describe it.[4]

We will begin with the longitudinal motion of a one-particle beam, i.e., a point charge Ne. Let z_n be the longitudinal displacement of the beam at the accelerating rf cavity in the nth revolution, measured relative to the synchronous particle. The rate of change of z_n is related to the relative energy error $\delta_n = \Delta E/E$ of the beam in the same nth revolution by Eq. (1.9), i.e.,

$$\frac{d}{dn} z_n = -\eta C \delta_n, \tag{4.1}$$

where η is the slippage factor defined in Eq. (1.10); C is the accelerator circumference. A positive z_n means the beam arrives at the rf cavity earlier than the synchronous particle. Again from Eq. (1.9), we have

$$\frac{d}{dn} \delta_n = \frac{(2\pi\nu_s)^2}{\eta C} z_n, \tag{4.2}$$

[1]Historically, the Vlasov equation technique was actually introduced earlier than the simplified models.

[2]That is, the lowest $m = 0$ cavity mode. In Figure 2.27, it corresponds to the tallest peak in Re $Z_0^{\parallel}$, which has the lowest resonant frequency.

[3]K. W. Robinson, Cambridge Electron Accel. Report CEAL-1010 (1964).

[4]M. Lee, SLAC Report SPEAR-31 (1970); Matthew Sands, Orsay LAL Reports 2-76, 3-76, 4-76 (1976); A. Hofmann, *Proc. Int. School Part. Accel.*, Erice, 1976, CERN Report 77-13, p. 139; P. B. Wilson, *AIP Proc.* **87**, *Phys. High Energy Accel.*, Fermilab, 1981, p. 450. One approach, adopted by Robinson but not in the present text, is to apply an equivalent circuit analysis. This is especially useful if one is interested not only in the beam dynamics but also the response of the rf system, the beam loading effect, and its feedback control.

where ν_s is the synchrotron tune. Typically, $\nu_s \ll 1$, i.e., the beam does not execute much synchrotron motion during the time it completes one revolution.

Equation (4.2) is valid when the beam has a vanishing intensity. For an intense beam, the energy variation also depends on the wake field generated by the beam. The $d\delta_n/dn$ equation then acquires an additional term,

$$\frac{d}{dn}\delta_n = \frac{(2\pi\nu_s)^2}{\eta C} z_n + \frac{eV(z_n)}{E}$$

$$= \frac{(2\pi\nu_s)^2}{\eta C} z_n - \frac{Nr_0}{\gamma} \sum_{k=-\infty}^{n} W_0'(kC - nC + z_n - z_k), \quad (4.3)$$

where W_0' is the longitudinal wake function accumulated over one turn of the accelerator. The summation over k is over the wake fields left behind by the beam from all revolutions previous to the nth. The argument of the wake function is the longitudinal separation of beam positions between the nth and the kth revolution. Combining Eqs. (4.1) and (4.3) yields the equation of motion

$$\frac{d^2 z_n}{dn^2} + (2\pi\nu_s)^2 z_n = \frac{Nr_0\eta C}{\gamma} \sum_{k=-\infty}^{n} W_0'(kC - nC + z_n - z_k). \quad (4.4)$$

In case the beam bunch has an oscillation amplitude much shorter than the wavelength of the fundamental cavity mode, one can expand the wake function:

$$W_0'(kC - nC + z_n - z_k) \approx W_0'(kC - nC) + (z_n - z_k) W_0''(kC - nC). \quad (4.5)$$

The first term on the right hand side of Eq. (4.5) is a static term independent of the motion of the beam. It describes the parasitic loss effect already discussed in Section 2.5 and can be taken care of by a constant shift in z_n. We will drop this term altogether. The second term, on the other hand, does involve the dynamics of the beam. The quantity $z_n - z_k$ is the difference of z's and—although we will not make such an approximation—resembles a time derivative dz/dn. An inspection of Eq. (4.4) then suggests an instability, since a dz/dn term in a d^2z/dn^2 equation indicates a possible exponential growth of z.

Substituting Eq. (4.5) into Eq. (4.4) gives a linear equation for z_n, which one can try to solve staying in the time domain. However, transforming to the

frequency domain at this point simplifies the mathematics considerably. In the frequency domain, z_n as a function of n is written as

$$z_n \propto e^{-in\Omega T_0}, \tag{4.6}$$

where $T_0 = C/c = 2\pi/\omega_0$ is the beam revolution period, and Ω is the mode frequency of the beam oscillation and is a key quantity yet to be determined. An ansatz of the form (4.6) is applicable only if the equation of motion is linear in z. By writing down Eq. (4.6), the problem of solving the differential equation of motion becomes the problem of solving an algebraic equation for Ω,

$$\Omega^2 - \omega_s^2 = -\frac{Nr_0\eta c}{\gamma T_0} \sum_{k=-\infty}^{\infty} (1 - e^{-ik\Omega T_0}) W_0''(kC), \tag{4.7}$$

where $\omega_s = \nu_s \omega_0$ is the synchrotron oscillation frequency and we have extended the summation over k to ∞ taking advantage of the causality property of the wake function.

The wake function can be expressed in terms of the longitudinal impedance using Eq. (2.72). An application of the identity from Eq. (2.210) then gives

$$\Omega^2 - \omega_s^2 = -i\frac{Nr_0\eta}{\gamma T_0^2} \sum_{p=-\infty}^{\infty} \left[p\omega_0 Z_0^{\parallel}(p\omega_0) - (p\omega_0 + \Omega) Z_0^{\parallel}(p\omega_0 + \Omega) \right]. \tag{4.8}$$

The factors $p\omega_0$ and $p\omega_0 + \Omega$ in front of $Z_0^{\parallel}$ come from taking the derivative of the induced voltage $V(z)$ with respect to z when we made the approximation (4.5). Given the impedance, Eq. (4.8) can in principle be solved for Ω. Here we will take a perturbative approach and assume Ω does not deviate much from ω_s for modest beam intensities. We thus replace Ω by ω_s on the right hand side of Eq. (4.8).

In general, Ω is complex. The real part of Ω is the perturbed synchrotron oscillation frequency of the collective beam motion, and the imaginary part gives the growth rate (or damping rate if negative) of the motion. Equation (4.8) then gives a *mode frequency shift*

$$\begin{aligned} \Delta\Omega &= \mathrm{Re}(\Omega - \omega_s) \\ &= \frac{Nr_0\eta}{2\gamma T_0^2 \omega_s} \sum_{p=-\infty}^{\infty} \left[p\omega_0 \,\mathrm{Im}\, Z_0^{\parallel}(p\omega_0) - (p\omega_0 + \omega_s) \mathrm{Im}\, Z_0^{\parallel}(p\omega_0 + \omega_s) \right] \end{aligned} \tag{4.9}$$

and an *instability growth rate*

$$\tau^{-1} = \mathrm{Im}(\Omega - \omega_s) = \frac{Nr_0\eta}{2\gamma T_0^2 \omega_s} \sum_{p=-\infty}^{\infty} (p\omega_0 + \omega_s)\mathrm{Re}\, Z_0^{\parallel}(p\omega_0 + \omega_s). \quad (4.10)$$

It is the imaginary part of the impedance that contributes to the collective frequency shift, and the real part that contributes to the instability growth rate.

There are two terms under the summation for $\Delta\Omega$ in Eq. (4.9). As we will show later in Eq. (6.59), the first term comes from a static phenomenon called *potential-well distortion*, while the origin of the second term is dynamical. Note that the growth rate τ^{-1} has a contribution only from the dynamical term. The static potential-well distortion does not contribute to τ^{-1}; mathematically, this term vanishes because $\mathrm{Re}\, Z_0^{\parallel}$ is an even function of ω.

It may be instructive at this point to make a detour to investigate why the impedance is sampled at the frequencies $p\omega_0$ and $p\omega_0 + \omega_s$ in Eqs. (4.9–4.10).[5] Consider first a point bunch circulating in the accelerator without synchrotron oscillation. The impedance will see the beam signal at times $t = kT_0$, i.e.,

$$\text{beam signal} \propto \sum_{k=-\infty}^{\infty} \delta(t - kT_0), \quad (4.11)$$

where the summation is over all revolutions; larger k means later revolutions. The frequency spectrum of the signal, obtained by a Fourier transformation, is

$$\begin{aligned} \text{spectrum} &\propto \int dt\, e^{i\omega t} \sum_{k=-\infty}^{\infty} \delta(t - kT_0) \\ &= \sum_{k=-\infty}^{\infty} e^{i\omega k T_0} = \omega_0 \sum_{p=-\infty}^{\infty} \delta(\omega - p\omega_0), \end{aligned} \quad (4.12)$$

where use has been made of Eq. (2.211). The frequency content of the beam signal is therefore a series of δ-functions at $\omega = p\omega_0$. This beam signal and spectrum are shown in Figure 4.1. For the static potential-well effect, the relevant signal seen by the impedance is therefore sampled at multiples of the revolution frequency $\omega = p\omega_0$.

[5] R. Littauer, *AIP Proc.* **105**, *Phys. High Energy Accel.*, SLAC, 1982, p. 869; S. Chattopadhyay, *AIP Proc.* **127**, *Phys. High Energy Accel.*, BNL/SUNY, 1983, p. 460; R. H. Siemann, *AIP Proc.* **184**, *Phys. Part. Accel.*, Fermilab 1987 and Cornell 1988, p. 430; J. Gareyte, *ibid.*, p. 343.

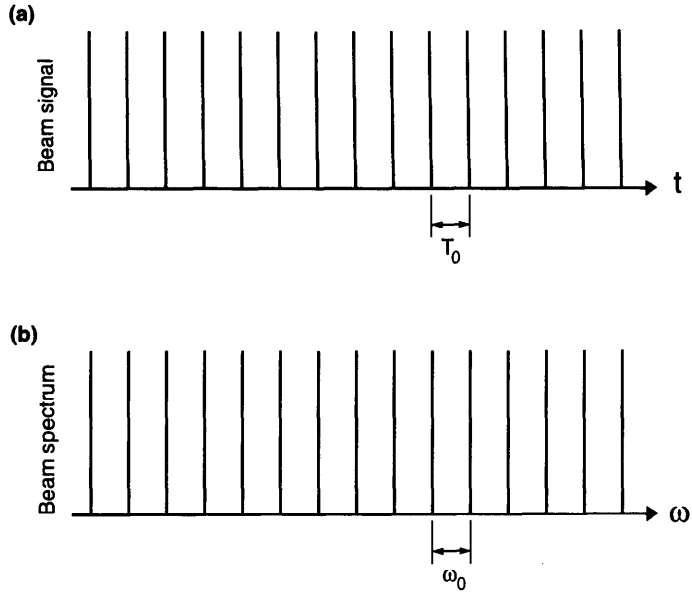

Figure 4.1. (a) Signal of a point-charge beam received by a pickup electrode or an impedance. (b) Spectrum of the signal in (a).

Exercise 4.1 The signal (4.11) is for a point-charge beam. For a beam with finite length, we have

$$\text{beam signal} \propto \sum_{k=-\infty}^{\infty} \rho(-ct + ckT_0), \tag{4.13}$$

where $\rho(z)$ is the bunch distribution ($z > 0$ is the bunch head). Show that the beam spectrum still consists of a series of δ-functions at frequencies $\omega = p\omega_0$, but the strengths of those δ-functions now contain an extra form factor of $\tilde{\rho}(\omega)$, given by Eq. (2.104), i.e.,

$$\text{spectrum} \propto \sum_{p=-\infty}^{\infty} \tilde{\rho}(p\omega_0)\delta(\omega - p\omega_0). \tag{4.14}$$

This beam signal and spectrum are shown in Figure 4.2 for a Gaussian beam. This additional form factor is the reason why the parasitic loss has the form of Eq. (2.212). It also says in order to obtain information on the

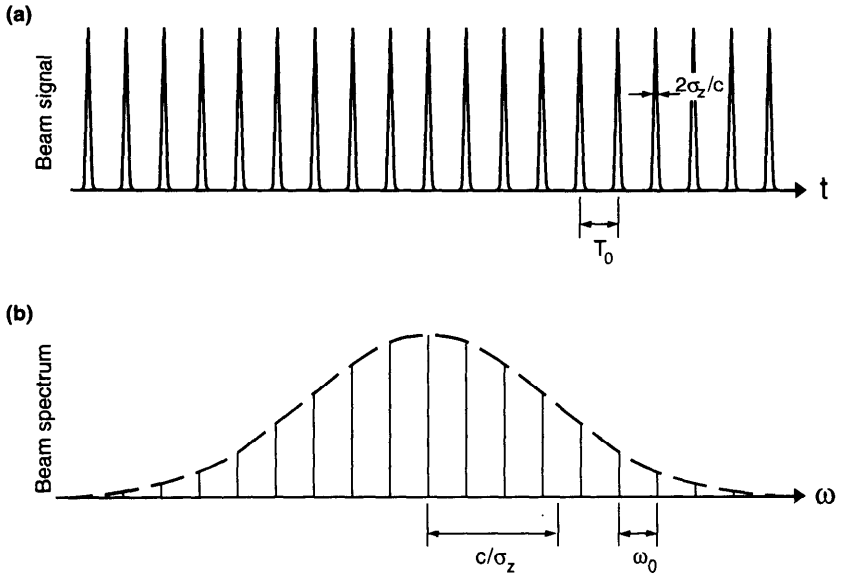

Figure 4.2. (a) Signal of a Gaussian beam, $\sigma_z / c = 0.05T_0$. (b) The spectrum of the Gaussian beam consists of a series of δ-functions like Figure 4.1(b), but also an additional Gaussian form factor whose rms width is $\sigma_\omega = c / \sigma_z$.

bunch length, a pickup must be sensitive to frequencies $p\omega_0 \gtrsim c/\sigma_z$, i.e., it must have a bandwidth $\gtrsim c/\sigma_z$.

We now let the point bunch execute a synchrotron oscillation, in which case we have

$$\text{beam signal} \propto \sum_{k=-\infty}^{\infty} \delta\left[t - kT_0 + \hat{\tau}\cos(\omega_s kT_0)\right], \tag{4.15}$$

where $\hat{\tau}$ is some small synchrotron oscillation amplitude. The frequency content of this signal is

$$\text{spectrum} \propto \sum_k e^{i\omega[kT_0 - \hat{\tau}\cos(\omega_s kT_0)]}. \tag{4.16}$$

For small oscillation amplitudes, this becomes

$$\text{spectrum} \propto \sum_k e^{i\omega kT_0}\left[1 - i\omega\hat{\tau}\cos(\omega_s kT_0)\right]. \tag{4.17}$$

Compared with Eq. (4.12), the spectrum contains a new term

$$
\begin{aligned}
&-i\omega\hat{\tau}\sum_k e^{i\omega kT_0}\cos(\omega_s kT_0) \\
&\quad = -\frac{i}{2}\omega\hat{\tau}\sum_k\left[e^{ikT_0(\omega+\omega_s)} + e^{ikT_0(\omega-\omega_s)}\right] \\
&\quad = -\frac{i}{2}\hat{\tau}\omega_0\sum_{p=-\infty}^{\infty}\left[(p\omega_0-\omega_s)\delta(\omega-p\omega_0+\omega_s)\right. \\
&\qquad\qquad \left.+(p\omega_0+\omega_s)\delta(\omega-p\omega_0-\omega_s)\right]. \qquad (4.18)
\end{aligned}
$$

The impedance responding to the synchrotron oscillation is therefore to be evaluated at $p\omega_0 \pm \omega_s$, i.e., the synchrotron sidebands of multiples of the revolution frequency. Equation (4.18) explains the form of the second terms of Eqs. (4.8–4.9), and Eq. (4.10).

Exercise 4.2 Consider the point-charge beam executing synchrotron oscillation and generating the signal of Eq. (4.15). In case the oscillation amplitude is not small, show that[5]

$$
\text{spectrum} \propto \sum_{l=-\infty}^{\infty}\sum_{p=-\infty}^{\infty} i^{-l}J_l\left[(p\omega_0+l\omega_s)\hat{\tau}\right]\delta(\omega-p\omega_0-l\omega_s). \qquad (4.19)
$$

Use Table 6.1 if necessary. The spectrum still consists of δ-functions. There is a set of δ-functions located at $\omega = p\omega_0$, whose amplitudes are proportional to $J_0(\omega\hat{\tau})$. For each p, there is a set of sidebands around $p\omega_0$, the lth sideband ($l = \pm$integers) occurs at $p\omega_0 + l\omega_s$, and their spectral strengths are proportional to $J_l(\omega\hat{\tau})$. This behavior is shown in Figure 4.3. For small $\hat{\tau}$, Eq. (4.19) becomes Eq. (4.18). What happens to the beam spectrum if the bunch has a finite length?

The Bessel function form factors mentioned in Exercise 4.2 come from the beam executing synchrotron oscillation. They are not to be confused with the form factor coming from the finite bunch length as discussed in Exercise 4.1. As we will see in Chapter 6, Bessel functions play an important role in the kinematics of collective modes, and the reason for their repeated appearance is embedded in the discussion in Exercise 4.2. The same Bessel form factors also appear in the frequency modulated (fm) signals for radios.

We now return to Eq. (4.10). Consider the resonator impedance of the form of Eq. (2.82) for the fundamental cavity mode. The only significant contributions to the growth rate (4.10) come from two terms in the summation, namely $p = \pm h$, assuming the width of the impedance peak $\omega_R/2Q$

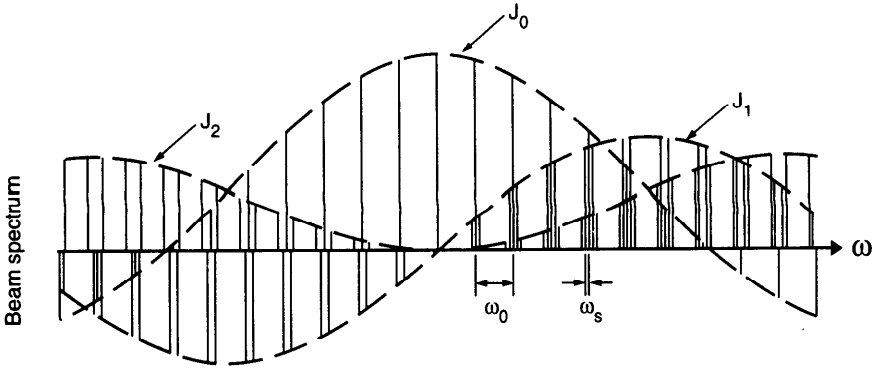

Figure 4.3. Spectrum of a point-charge beam which is synchrotron oscillating with frequency $\omega_s = \omega_0 / 10$ and an exaggerated amplitude of $\hat{\tau} = 1 / 3\,\omega_0$. Around each $p\omega_0$, there is a cluster of sidebands spaced by ω_s. Each sideband is specified by one index l, and the lth sideband has a strength proportional to $J_l[(p\omega_0 + l\omega_s)\hat{\tau}]$. Sidebands up to $l = \pm 2$ are shown.

and the synchrotron frequency ω_s are both much less than ω_0. This gives

$$\tau^{-1} \approx \frac{Nr_0\eta h\omega_0}{2\gamma T_0^2\omega_s}\left[\mathrm{Re}\, Z_0^{\parallel}(h\omega_0 + \omega_s) - \mathrm{Re}\, Z_0^{\parallel}(h\omega_0 - \omega_s)\right]. \quad (4.20)$$

Beam stability requires $\tau^{-1} \leq 0$. That is, the real part of the impedance must be lower at frequency $h\omega_0 + \omega_s$ than at frequency $h\omega_0 - \omega_s$ if $\eta > 0$ (above transition), and the other way around if $\eta < 0$ (below transition). This condition implies the *Robinson criterion* that, above transition, the resonant frequency ω_R of the fundamental cavity mode should be slightly detuned downwards from an exact integral multiple of ω_0. Below transition, stability requires ω_R be slightly higher than $h\omega_0$. The situation is illustrated in Figure 4.4. When the Robinson criterion is met, the synchrotron oscillation of the beam is "Robinson damped," and this damping will help in stabilizing the beam against similar instabilities due to other impedance sources.

Substituting Eq. (2.82) into Eq. (4.20) and assuming that both ω_s and $\Delta\omega = \omega_R - h\omega_0$ are much less than the resonator width $\omega_R/2Q$ which, in turn, is much less than ω_0, we obtain

$$\tau^{-1} \approx \frac{4Nr_0\eta R_S Q^2\,\Delta\omega}{\pi\gamma T_0 h}. \quad (4.21)$$

Similarly we have

$$\Delta\Omega \approx -\frac{12Nr_0\eta R_S Q^3\nu_s\,\Delta\omega}{\pi\gamma T_0 h^2}. \quad (4.22)$$

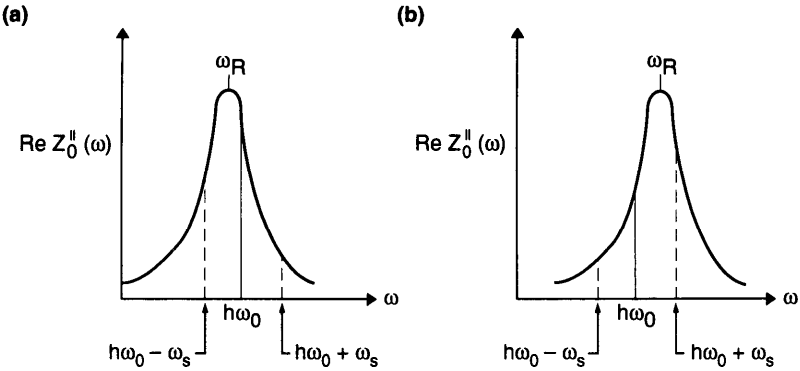

Figure 4.4. Illustration of the Robinson stability criterion. The rf fundamental mode is detuned so that ω_R is (a) slightly below $h\omega_0$ and (b) slightly above $h\omega_0$. (a) is Robinson damped above transition and antidamped below transition. (b) is antidamped above transition and damped below transition.

Taking for example $\eta = 0.03$ (above transition), $N = 10^{11}$, $E = 1$ GeV,[6] $\omega_0 = 9.4 \times 10^6\ \mathrm{s}^{-1}$, $\nu_s = 0.01$, $h\omega_0/2\pi = 360$ MHz, $R_S = 1\ \mathrm{M}\Omega$, $Q = 2000$, $\Delta\omega/2\pi = -10$ kHz (rf detuned lower for stability), $h = 240$, we find $\tau = -1.2$ ms and $\Delta\Omega = 0.2 \times 10^3\ \mathrm{s}^{-1}$. Robinson damping (or antidamping) can be rather strong. Figure 4.5 gives the numerical results obtained by inserting the resonator impedance (2.82) into Eqs. (4.9) and (4.10) and their comparison with the approximate expressions (4.21) and (4.22).

Physically, Robinson instability comes from the fact that the revolution frequency of an off-momentum beam is not given by ω_0 but by $\omega_0(1 - \eta\delta)$. To illustrate the Robinson instability mechanism, consider a beam executing synchrotron oscillation above transition. Due to the energy error of the beam, the impedance samples the beam signal at a frequency slightly below $h\omega_0$ if $\delta > 0$, and slightly above $h\omega_0$ if $\delta < 0$. In order to damp this synchrotron oscillation of the beam, we need to let the beam lose energy when $\delta > 0$ and gain energy when $\delta < 0$ (at least relative to the case when $\delta = 0$). This can be achieved by having an impedance that decreases with increasing frequency in the neighborhood of $h\omega_0$. The Robinson criterion then follows.

Although the Robinson instability was originally considered for the fundamental mode of the rf cavities, it is obvious that the same analysis applies to the higher rf modes, in which case we would pay attention to accidentally landing the frequencies $p\omega_0$ for some integer p on the wrong side of some higher order impedance peak. Since there are typically many higher order modes for a given rf cavity design, it is sometimes necessary to damp them by

[6]This is meant to be the particle energy at injection. In a circular accelerator, it is usually during the low energy operation that the beam is least stable. The beam usually becomes more stable when accelerated to higher energies.

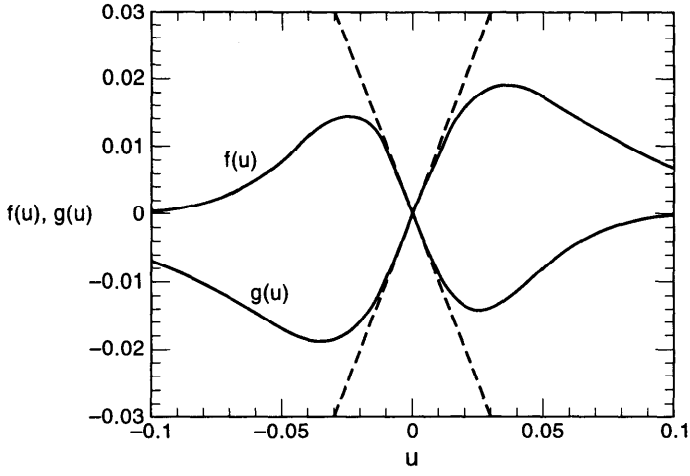

Figure 4.5. The collective mode frequency shift $\Delta\Omega = (3Q\nu_s\xi / h)f(\upsilon)$ and growth rate $\tau^{-1} = \xi g(\upsilon)$ due to a resonator impedance are shown as functions of the detuning $\upsilon = (\omega_R - h\omega_0) / \omega_0$. We have defined $\xi = 8Nr_0\eta R_S Q^2 / \gamma T_0^2 h$. For small $\omega_s \ll \omega_R / 2Q$, the maximum Robinson damping and antidamping occur when $\upsilon = \pm h / 2\sqrt{3}Q$. The dashed curves are the approximate expressions (4.21 – 4.22), or $f(\upsilon) \approx -\upsilon$ and $g(\upsilon) \approx \upsilon$. We have taken $h = 240$, $Q = 2000$, and $\nu_s = 0.01$.

a careful design in order to assure beam stability.[7] As a rough estimate of the maximum growth rate due to a higher order cavity mode, one may substitute $\Delta\omega \approx \pm\omega_R / 2\sqrt{3}Q$ (the worst case) into Eq. (4.21). Often in practice a proper detuning of the fundamental mode frequency will overcome the contributions from the accidental higher order modes.

Note that Eqs. (4.9) and (4.10) apply also to impedances other than the rf impedance. The space charge impedance (2.80), for example, being purely imaginary, causes a collective frequency shift but not an instability. However, substituting Eq. (2.80) into Eq. (4.9) or substituting the resistive-wall impedance (2.76) into Eqs. (4.9–4.10) leads to divergent results. These are consequences of the point-charge assumption. When a more realistic bunch distribution is used, the bunch spectrum will cut off the high-frequency divergences, yielding physically meaningful results. These will be elaborated further in Section 6.3.

To generalize the context further, it should be mentioned that the Robinson analysis does not have to be restricted to longitudinal effects. A similar analysis, given in the next section, for the transverse $m = 1$ wake fields leads to a "transverse Robinson" effect. Furthermore, as will be discussed in Chapter 6, by allowing internal degrees of freedom in the beam, higher bunch modes—so far excluded from the analysis because we assumed

[7]This involves the *de-Q*-ing of those higher order rf cavity modes. See further discussions following Eq. (4.32).

a one-particle model—also have their own versions of longitudinal and transverse Robinson instability and their corresponding stability criteria.

In case the longitudinal impedance is broad-banded in such a way that there are no fine structures of frequency width $\lesssim \omega_0$, the summation Σ_p in Eq. (4.10) can be approximated by $\int dp$. The fact that $\mathrm{Re}\, Z_0^{\parallel}$ is an even function of ω leads to the important conclusion that broad-band impedances (or equivalently, short range wake fields) do not cause instabilities of the Robinson type characterized by Eq. (4.10). This point will be elaborated further in Section 6.5.

Exercise 4.3 So far we have been considering a circulating beam with a single bunch.

(a) Follow steps similar to those in the text to set up the problem for a beam with two bunches, each with charge Ne and located diametrically opposite on the circumference. Show that there are two modes of collective motions, whose complex mode frequencies are

$$\Omega_{\pm} - \omega_s \approx -i\frac{Nr_0\eta}{2\gamma T_0^2\omega_s}\sum_{p=\infty}^{\infty}\Big\{\big[1+(-1)^p\big]p\omega_0 Z_0^{\parallel}(p\omega_0) - \big[1\pm(-1)^p\big](p\omega_0+\omega_s)Z_0^{\parallel}(p\omega_0+\omega_s)\Big\}. \quad (4.23)$$

Use Eq. (4.23) to show that the Robinson stability criterion remains the same as in the single-bunch case for a sharp rf fundamental mode. What happens if the two bunches have slightly different ω_s? How about slightly different intensities? [Hint: Refer to Section 4.6 if necessary. For the case with two bunches, the harmonic number h must be an even number].

(b) How, if at all, is the Robinson criterion modified if the two bunches have charges Ne and $-Ne$ and circulate in opposite directions around the accelerator?

4.2 RIGID BEAM TRANSVERSE INSTABILITY

We now consider a one-particle beam executing a transverse betatron oscillation, say in the vertical y-direction. The beam possesses an instantaneous dipole moment $Ney(s)$. A particle that follows the beam at a distance d behind sees, according to Table 2.2, a vertical wake force

$$-Ne^2y(s)W_1(-d)/C.$$

The equation of motion of the one-particle beam is

$$y''(s) + \left(\frac{\omega_\beta}{c}\right)^2 y(s) = -\frac{Nr_0}{\gamma C}\sum_{k=1}^{\infty} y(s-kC)W_1(-kC), \quad (4.24)$$

where a prime on $y(s)$ means taking derivative with respect to s, W_1 is the wake function integrated around the accelerator circumference C,[8] and the summation over k sums the wake fields over all previous revolutions. This model was first suggested by Courant and Sessler,[9] and also by Ferlenghi, Pellegrini, and Touschek.[10]

Of course, an off-axis beam also possesses distribution moments other than the dipole moment. For instance, it possesses a monopole moment (i.e., the total beam charge) and higher moments such as the quadrupole moment. The monopole moment has been considered in Section 4.1 and in any case does not give rise to a transverse wake force. Effects due to the higher moments can be ignored as compared with the dipole wake effects if we assume the beam displacement y is much smaller than the vacuum chamber pipe radius.

One may still object that a dipole moment also generates a longitudinal wake, which is not considered in Eq. (4.24). Indeed, strictly speaking, a rigorous treatment of the problem must also include the longitudinal motion of the beam. Thus, the transverse wake force in the betatron equation of motion (4.24) should be modulated by the arrival time of the beam, while the synchrotron motion should be perturbed by the betatron motion through the longitudinal wake W_1'. Only when this coupled synchro-betatron motion is considered does the system strictly satisfy the Maxwell equations and become fully Hamiltonian. However, for practical purposes, as long as the synchrotron and betatron frequencies are not close to a resonance condition $\omega_\beta \pm \omega_s = n\omega_0$ (where $\omega_0 = 2\pi c/C = 2\pi/T_0$) and the transverse displacements are small, Eq. (4.24) still accurately describes the transverse motion of the beam. We will return to this point following Eq. (6.162).

We again solve Eq. (4.24) in the frequency domain. Letting $y \propto \exp(-i\Omega s/c)$ and transforming the wake function into the transverse impedance, we obtain the following equation for the complex mode frequency Ω,

$$\Omega^2 - \omega_\beta^2 = \frac{Nr_0 c}{\gamma T_0} \sum_{k=1}^{\infty} e^{ik\Omega T_0} W_1(-kC)$$

$$= -i\frac{Nr_0 c}{\gamma T_0^2} \sum_{p=-\infty}^{\infty} Z_1^{\perp}(p\omega_0 + \Omega), \tag{4.25}$$

where $Z_1^{\perp}$ is the total impedance around the accelerator circumference.

[8] In the present approximation, it does not matter if the impedance is localized or distributed around the circumference. See discussion following Eq. (1.16).

[9] Ernest D. Courant and Andrew M. Sessler, *Rev. Sci. Instr.* **37**, 1579 (1966).

[10] E. Ferlenghi, C. Pellegrini, and B. Touschek, *Nuovo Cimento* **44B**, 253 (1966); C. Pellegrini, *Physics with Intersecting Storage Rings*, Enrico Fermi Int. School of Phys., Academic Press, New York, 1971, p. 221.

The structure of Eq. (4.25) can be understood by observing that

$$\Delta\nu_y \sim \frac{\beta_y}{4\pi}\left(\frac{-ieIZ_1^{\perp}}{E}\right), \tag{4.26}$$

where $\Delta\nu_y = (\Omega - \omega_\beta)/\omega_0$ is the mode tune shift, $\beta_y = R/\nu_y$ is the β-function, and $-iIZ_1^{\perp}$ is the transverse voltage per unit vertical displacement. At a fundamental level, the quantity $\Delta\nu_y$ is just the tune shift as described in Eqs. (1.13–1.16), except that the perturbation now comes from the collective wake forces instead of errors in the external focusing force, and that the resultant frequency shift is complex in general.

In contrast with Eqs. (4.8–4.10), the transverse case does not contain a potential-well distortion term. This is a consequence of the fact that, given the wake field established in previous revolutions, the transverse force on the macroparticle beam does not depend on the instantaneous transverse displacement of the beam. In other words, the transverse $m = 1$ wake field does not form a potential well.

Assuming Ω does not deviate much from ω_β so that Ω on the right hand side of Eq. (4.25) can be replaced by ω_β, we have a mode frequency shift

$$\Delta\Omega = \mathrm{Re}(\Omega - \omega_\beta) \approx \frac{Nr_0c}{2\gamma T_0^2\omega_\beta}\sum_{p=-\infty}^{\infty} \mathrm{Im}\, Z_1^{\perp}(p\omega_0 + \omega_\beta) \tag{4.27}$$

and growth rate

$$\tau^{-1} = \mathrm{Im}(\Omega - \omega_\beta) \approx -\frac{Nr_0c}{2\gamma T_0^2\omega_\beta}\sum_{p=-\infty}^{\infty} \mathrm{Re}\, Z_1^{\perp}(p\omega_0 + \omega_\beta). \tag{4.28}$$

The reason the impedance is sampling the frequencies $p\omega_0 + \omega_\beta$ follows from a consideration similar to that following Eq. (4.11). In the present case,

$$\text{beam signal} \propto \sum_{k=-\infty}^{\infty} \delta(t - kT_0)\,\hat{y}e^{-i\omega_\beta t}, \tag{4.29}$$

where $\hat{y}$ is some betatron oscillation amplitude. The spectrum seen by the impedance is the Fourier transformation of Eq. (4.29),

$$\text{spectrum} \propto \hat{y}\omega_0 \sum_{p=-\infty}^{\infty} \delta(\omega - p\omega_0 - \omega_\beta). \tag{4.30}$$

The impedance therefore responds to frequencies $\omega = p\omega_0 + \omega_\beta$, i.e., the betatron sidebands of multiples of the revolution frequency.

Given the transverse impedance, Eqs. (4.27–4.28) are our main results. They are the transverse counterparts of the longitudinal Robinson instability effect. The real and the imaginary parts of the impedance contribute to the instability growth rate and the collective frequency shift, respectively, just as in the longitudinal Robinson case. In particular, for the case of space charge, the purely imaginary impedance gives rise to only a mode frequency shift and not an instability growth.

If the real part of $Z_1^{\perp}(\omega)$ contains sharp resonant peaks, there can be a *transverse Robinson instability*. More explicitly, if a resonant frequency ω_R is close to $h\omega_0$, an integral multiple of ω_0, then

$$\tau^{-1} \approx -\frac{Nr_0c}{2\gamma T_0^2\omega_\beta}\left[\operatorname{Re} Z_1^{\perp}(h\omega_0 + \Delta_\beta\omega_0) - \operatorname{Re} Z_1^{\perp}(h\omega_0 - \Delta_\beta\omega_0)\right], \quad (4.31)$$

where Δ_β is the noninteger part of the betatron tune $\nu_\beta = \omega_\beta/\omega_0$ and we have chosen $-\frac{1}{2} < \Delta_\beta < \frac{1}{2}$. A positive Δ_β means ν_β is above an integer; a negative Δ_β means ν_β is below an integer. For stability, ω_R should be slightly above $h\omega_0$ if $\Delta_\beta > 0$ and below $h\omega_0$ if $\Delta_\beta < 0$. The stability criterion of the transverse Robinson instability does not depend on whether the accelerator is operated above or below transition. Instead, it depends on whether the betatron tune is above or below an integer.

For a sharp resonator impedance whose resonant frequency ω_R happens to be close to $h\omega_0$, and assuming that both $|\omega_R - h\omega_0|$ and $|\Delta_\beta\omega_0|$ are much less than $\omega_R/2Q$, which is in turn much less than ω_0, we have

$$\begin{aligned} \Delta\Omega &\approx -\frac{Nr_0c^2R_SQ}{2\pi^2\gamma\omega_\beta h^2}(\omega_R - h\omega_0), \\ \tau^{-1} &\approx -\frac{2Nr_0c^2R_SQ^2}{\pi^2\gamma\omega_\beta h^3}(\omega_R - h\omega_0)\Delta_\beta. \end{aligned} \quad (4.32)$$

As a numerical example, let $N = 10^{11}$, $R_S = 40\ \mathrm{M\Omega/m^2}$, $Q = 2000$, $E = 1$ GeV (electron beam), $\omega_0 = 9.4 \times 10^6\ \mathrm{s^{-1}}$, $\nu_\beta = 6.05$, $h = 518$, and $(\omega_R - h\omega_0)/\omega_0 = \pm h/2\sqrt{3}Q$ (the worst case). We find $\tau = \mp 5$ ms and $\Delta\Omega = \mp 260\ \mathrm{s^{-1}}$. Figure 4.6 shows the mode frequency shift and the growth rate as functions of $\omega_R - h\omega_0$.

Since the exact values of all the transverse cavity mode frequencies are not easy to control, the value of ω_R of a transverse cavity mode is equally likely to be above or below $h\omega_0$ for some integer h; this collective beam motion is equally likely to be damped or antidamped.[11] In designing an accelerator for

[11]A statistical analysis can be found in C. Pellegrini and M. Sands, SLAC Report PEP-258 (1977); R. Siemann, *IEEE Trans. Nucl. Sci.* **NS-28**, 2437 (1981).

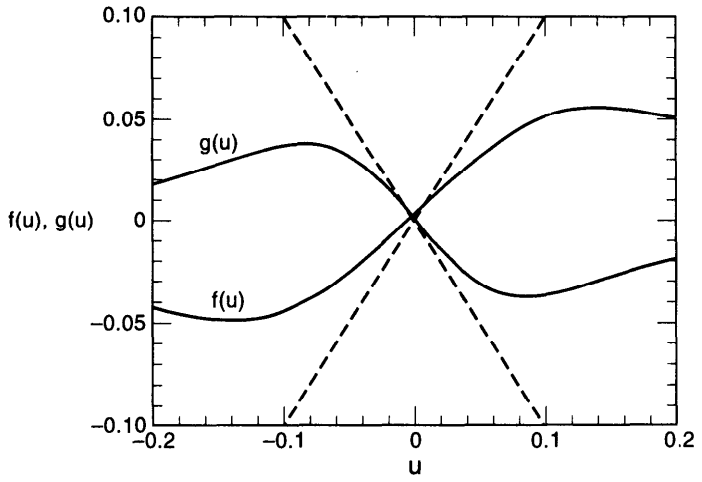

Figure 4.6. Mode frequency shift $-\xi f(\upsilon)$ and growth rate $(4Q\Delta_\beta \xi / h)g(\upsilon)$ as functions of $\upsilon = (\omega_R - h\omega_0)/\omega_0$, where $\xi = Nr_0c^2R_SQ / 2\pi^2\gamma\nu_\beta h^2$. For small $\Delta_\beta \ll h / 2Q$, maximum damping and antidamping occur when $\upsilon = \pm h / 2\sqrt{3}Q$. The dashed curves are the approximate expressions (4.32), which correspond to $f(\upsilon) \approx \upsilon$ and $g(\upsilon) \approx -\upsilon$. The parameters chosen are $\Delta_\beta = 0.05$, $Q = 2000$, $h = 518$. The dependence on Δ_β is weak as long as it is much less than $h / 2Q$.

high intensity beams, therefore, it is often necessary to *de-Q* the higher order modes by either passively or actively removing their field energies from the rf cavities. The higher order mode field energy often needs to be reduced by one or two orders of magnitude before the next beam bunch comes along. This is a demanding technology[12] because, among other considerations, the higher order modes must be de-*Q*ed without significantly affecting the operation of the cavity fundamental mode. By reducing the *Q*-value of the higher order modes sufficiently, the growth rates are reduced and the remaining collective instability can be handled by a conventional feedback system.

Unlike its longitudinal counterpart, the transverse Robinson instability does not have the strong damping provided by the fundamental rf cavity mode (assumed properly tuned), which makes it more of a serious concern. In principle, one could obtain a transverse Robinson damping by intentionally introducing an rf cavity whose resonator impedance is near $\omega_R \approx h\omega_0$ and tuning it favorably to counteract the accidental modes.

In case of a broad-band impedance (short range wake field), the summation over p can be approximated by an integral over p. It then follows from Eq. (4.28) and the fact that $\mathrm{Re}\, Z_1^\perp$ is an odd function of frequency

[12]R. Klatt and T. Weiland, DESY Report M-84-06 (1984); R. Palmer, SLAC-PUB-4542 (1989); H. Padamsee et al., *AIP Proc.* **214**, *Beam Dynamics Issues of High-Luminosity Asymmetric Collider Rings*, Berkeley, 1990, p. 235.

that $\tau^{-1} = 0$.[13] Broad-band impedances therefore do not cause transverse Robinson instability, a situation similar to the longitudinal case. However, as will be explained later in Sections 4.5 and 6.7, a broad-band impedance does cause an instability when the betatron frequency of a particle is not a constant, as assumed so far, but depends on its relative energy deviation δ.

Exercise 4.4 Using Eq. (4.28), show that the instability growth rate $\tau^{-1} = 0$ if ν_β = integer or if ν_β = integer + $\frac{1}{2}$. This is true for an arbitrary impedance.

As another application of the analysis of this section, let us find the instability growth rate and mode frequency shift for an accelerator with a resistive vacuum chamber. Substituting the transverse wake function (2.53) into Eq. (4.25), we obtain the result[14]

$$\tau^{-1} \approx -\frac{Nr_0c^2}{b^3\gamma\omega_\beta T_0\sqrt{\pi\sigma\omega_0}} f(\Delta_\beta),$$
$$f(\Delta_\beta) = \sum_{k=1}^{\infty} \sqrt{\frac{2}{k}} \sin(2\pi k\Delta_\beta), \tag{4.34}$$

and

$$\Delta\Omega \approx -\frac{Nr_0c^2}{b^3\gamma\omega_\beta T_0\sqrt{\pi\sigma\omega_0}} g(\Delta_\beta),$$
$$g(\Delta_\beta) = \sum_{k=1}^{\infty} \sqrt{\frac{2}{k}} \cos(2\pi k\Delta_\beta). \tag{4.35}$$

The functions $f(\Delta_\beta)$ and $g(\Delta_\beta)$ are depicted in Figure 4.7. We see that $f(\Delta_\beta)$ is positive (so that $\tau^{-1} < 0$ and the beam is stable) if $0 < \Delta_\beta < \frac{1}{2}$, and negative if $-\frac{1}{2} < \Delta_\beta < 0$. This means one should choose the betatron tune above an integer to assure stability against the resistive-wall wake fields. This is to be compared with the case of the resonator impedance, Eq. (4.31), for which the stability condition on Δ_β depends on the sign of $\omega_R - h\omega_0$.

[13]Incidentally, one would also expect $\Delta\Omega = 0$ for a broad-band impedance because $W_1(0) = 0$, i.e., the one-particle beam does not see its own wake force. This is indeed true by replacing $\Sigma_p \to \int dp$ in Eq. (4.27) and observing Eq. (2.93).

[14]One could also obtain Eq. (4.34) by inserting the impedance (2.76) into Eq. (4.28). This leads to another expression for $f(\Delta_\beta)$, i.e.,

$$f(\Delta_\beta) = \frac{1}{\sqrt{2}} \sum_{p=-\infty}^{\infty} \frac{\operatorname{sgn}(p + \Delta_\beta)}{|p + \Delta_\beta|^{1/2}}. \tag{4.33}$$

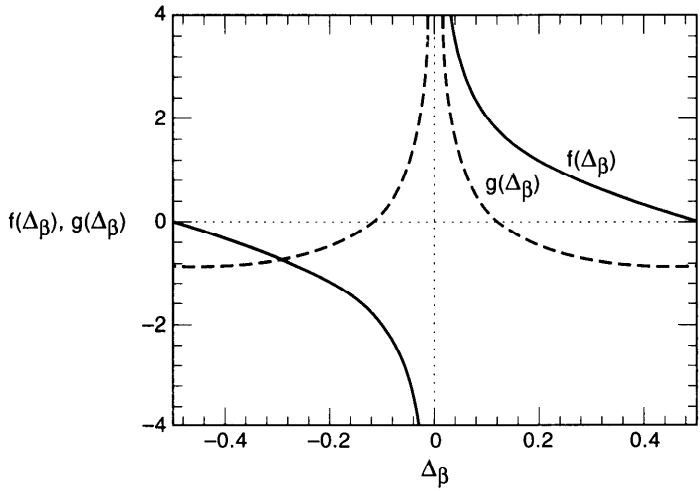

Figure 4.7. The functions $f(\Delta_\beta)$ and $g(\Delta_\beta)$ of Eqs. (4.34 – 4.35) are given as solid and dashed curves, respectively.

Take for example, $N = 10^{11}$, $b = 5$ cm, $E = 1$ GeV (electron beam), $\nu_\beta = 5.9$ (below an integer; therefore the beam is unstable), $\omega_0 = 9.4 \times 10^6$ s^{-1}, and $\sigma = 3 \times 10^{17}$ s^{-1}. We find $f(\Delta_\beta) = -2.0$ and an instability growth time of $\tau = 0.5$ s.

It will be shown later by Eq. (5.90) that, because the resistive-wall instability is rather weak, a small spread of betatron tune of the particles in the beam will stabilize the beam even if the betatron tune is below an integer. In practice, therefore, the choice of betatron tune is most likely not seriously restricted by the resistive-wall effect.

The stability criterion invariably involves the sign of Δ_β. This is because the beam oscillation is damped or antidamped depending on the relative phase between the beam oscillation and the wake force induced by the beam oscillation (damped if the wake force lags the beam oscillation and antidamped if the wake force leads the beam oscillation, much like what a child does when playing a swing set), and the relative phase is determined by Δ_β in the multiturn stability being considered.

4.3 STRONG HEAD-TAIL INSTABILITY

In Section 3.2, we treated the dipole beam breakup effect in linacs. There is also a dipole beam breakup mechanism in a circular accelerator; it will be called the *strong head-tail instability* here.[15] It is sometimes also called the

[15]The modifier "strong" is to distinguish this instability mechanism from that to be mentioned in Section 4.5.

transverse mode coupling instability, the transverse turbulent instability, or the transverse microwave instability in the literature.[16] The difference from the linac case is that now the beam particles are no longer frozen in their relative longitudinal positions. Instead, they execute synchrotron oscillations, thus constantly changing their relative longitudinal positions, with a low frequency ω_s.

To illustrate the mechanism of the strong head-tail instability, consider a two-particle beam that is made of two macroparticles, each with charge of $Ne/2$ and each executing synchrotron oscillation. We assume their synchrotron oscillations have equal amplitude but opposite phases. During time $0 < s/c < T_s/2$, where $T_s = 2\pi/\omega_s$ is the synchrotron oscillation period, particle 1 leads particle 2; the equations of motion for the two macroparticles are

$$\begin{aligned} y_1'' + \left(\frac{\omega_\beta}{c}\right)^2 y_1 &= 0, \\ y_2'' + \left(\frac{\omega_\beta}{c}\right)^2 y_2 &= \frac{Nr_0 W_0}{2\gamma C} y_1. \end{aligned} \tag{4.36}$$

Similarly, during $T_s/2 < s/c < T_s$, we have the same equations with indices 1 and 2 exchanged. Then during $T_s < s/c < 3T_s/2$, Eq. (4.36) applies again, etc. The quantities y_1 and y_2 are considered to be infinitesimal initially. Whether the beam is stable depends on their behavior in time. If the beam is stable, they will remain infinitesimal. If the beam is unstable, they will grow exponentially with time. This model was first suggested by Kohaupt[17] and Talman.[18]

In writing down Eq. (4.36), we have assumed for simplicity that the wake function (integrated over the accelerator circumference C), $W_1(z)$, is a constant, and yet it vanishes before the beam completes one revolution, i.e.,

$$W_1(z) = \begin{cases} -W_0 & \text{if } 0 > z > -(\text{bunch length}), \\ 0 & \text{otherwise.} \end{cases} \tag{4.37}$$

The property of wake functions requires that $W_0 > 0$. The short range wake function of (4.37) corresponds to an impedance which is broad-banded. In contrast with the Robinson-type instabilities, the strong head-tail instability is essentially a single-turn phenomenon.

[16]The latter two terms tend to imply instabilities involving higher order collective modes not properly represented by a two-particle model, but this subtlety is not important for our purpose here.

[17]R. D. Kohaupt, DESY Report M-80/19 (1980).

[18]R. Talman, CERN Report ISR-TH/81-17 (1981); R. Talman, *Nucl. Instr. Meth.* **193**, 423 (1982).

We now analyze the stability condition of the two-particle beam system. From Eq. (4.36), the solution for y_1 is simply a free betatron oscillation,

$$\tilde{y}_1(s) = \tilde{y}_1(0)e^{-i\omega_\beta s/c}, \tag{4.38}$$

where

$$\tilde{y}_1 = y_1 + i\frac{c}{\omega_\beta}y_1'. \tag{4.39}$$

Both the real and imaginary parts are meaningful in the representation (4.38–4.39).

Substituting Eq. (4.38) into the equation for y_2 yields the solution

$$\tilde{y}_2(s) = \tilde{y}_2(0)e^{-i\omega_\beta s/c} + i\frac{Nr_0W_0c}{4\gamma C\omega_\beta}\left[\frac{c}{\omega_\beta}\tilde{y}_1^*(0)\sin\frac{\omega_\beta s}{c} + \tilde{y}_1(0)se^{-i\omega_\beta s/c}\right]. \tag{4.40}$$

There are three terms in Eq. (4.40). The first two terms describe the free betatron oscillation; the third term, proportional to s, is the resonantly driven response. Equation (4.40) has its linac counterpart given by Eq. (3.24).

Equation (4.40) can be simplified if $\omega_\beta T_s/2 \gg 1$, or equivalently, $\omega_\beta \gg \omega_s$. In that case, the second term on the right hand side of Eq. (4.40) can be dropped because it is much smaller than the third term, and we can write the solution for the equations of motion during the period $0 < s/c < T_s/2$ in a matrix form,

$$\begin{bmatrix}\tilde{y}_1\\ \tilde{y}_2\end{bmatrix}_{s=cT_s/2} = e^{-i\omega_\beta T_s/2}\begin{bmatrix}1 & 0\\ i\Upsilon & 1\end{bmatrix}\begin{bmatrix}\tilde{y}_1\\ \tilde{y}_2\end{bmatrix}_{s=0}, \tag{4.41}$$

where [cf. Eq. (3.25)] we have defined a positive, dimensionless parameter

$$\Upsilon = \frac{\pi Nr_0W_0c^2}{4\gamma C\omega_\beta\omega_s}. \tag{4.42}$$

The time evolution during $T_s/2 < s/c < T_s$ can be obtained by exchanging indices 1 and 2 in the above analysis. The total transformation for one full synchrotron period is therefore

$$\begin{aligned}\begin{bmatrix}\tilde{y}_1\\ \tilde{y}_2\end{bmatrix}_{cT_s} &= e^{-i\omega_\beta T_s}\begin{bmatrix}1 & i\Upsilon\\ 0 & 1\end{bmatrix}\begin{bmatrix}1 & 0\\ i\Upsilon & 1\end{bmatrix}\begin{bmatrix}\tilde{y}_1\\ \tilde{y}_2\end{bmatrix}_0\\ &= e^{-i\omega_\beta T_s}\begin{bmatrix}1-\Upsilon^2 & i\Upsilon\\ i\Upsilon & 1\end{bmatrix}\begin{bmatrix}\tilde{y}_1\\ \tilde{y}_2\end{bmatrix}_0.\end{aligned} \tag{4.43}$$

As time evolves, the vector formed by the phasors $\tilde{y}_1$ and $\tilde{y}_2$ is repeatedly transformed by the 2×2 matrix in Eq. (4.43). Stability of the system is thus determined by the eigenvalues of this matrix. The two eigenvalues for the two modes (a + mode and a − mode) are

$$\lambda_{\pm} = e^{\pm i\phi}, \qquad \sin\frac{\phi}{2} = \frac{\Upsilon}{2}, \tag{4.44}$$

and the eigenvectors are

$$V_{\pm} = \begin{bmatrix} \pm e^{\pm i\phi/2} \\ 1 \end{bmatrix}. \tag{4.45}$$

Stability requires ϕ real, which is fulfilled if $|\sin(\phi/2)| \leq 1$, or

$$\Upsilon \leq 2. \tag{4.46}$$

For weak beams, $\Upsilon \ll 1$, we have $\phi \approx \Upsilon$. Near the instability, ϕ approaches π as Υ approaches 2.

An inspection of Eq. (4.41) indicates that the instability that occurs when $\Upsilon > 2$ causes a rather severe disruption of the beam, as seen by the fact that, during half a synchrotron period, the motion of the trailing particle has grown by an amount more than twice the amplitude of the free-oscillating leading particle. For $\Upsilon \leq 2$, the growths made during the half synchrotron periods when the particle is trailing do not accumulate and the beam is stable. As the beam intensity increases so that $\Upsilon > 2$, the growths of the particles then do accumulate and bootstrap into an instability. This *threshold* behavior is very different from the linac case, in which the beam—at least its tail—is always unstable. One can imagine that, by periodically exchanging the roles of leading and trailing particles, the two-particle beam is made more stable. The more frequently they are exchanged, the more stable is the beam. This shows up in the fact that Υ is inversely proportional to ω_s. Synchrotron oscillation is thus an effective stabilizing mechanism in circular accelerators. Strong betatron focusing and a high beam energy also help stabilize the beam, as indicated by the fact that Υ is inversely proportional to γ and ω_β. The factor $1/\omega_\beta$ in Υ is related to the β-function. If the β-function β_Z at the location of the impedance is known, a better expression for Υ would be obtained by replacing c/ω_β by β_Z.

In an accelerator, the most readily available beam signal comes from the beam position monitors that measure the center of charge of the beam. In the two-particle model, the center-of-charge signal is given by $y_1 + y_2$. In particular, it will be useful to examine its frequency spectrum. To do that, consider a two-particle beam that is in a pure eigenstate $V_{\pm}$ at time $s/c = 0$. In the stable region, it is straightforward to show that the subsequent motion

of the beam center of charge is given by

$$(\tilde{y}_1 + \tilde{y}_2)(s) = \exp\left[-i\left(\omega_\beta \mp \frac{\phi\omega_s}{2\pi}\right)\frac{s}{c}\right]\sum_{l=-\infty}^{\infty} C_l e^{-il\omega_s s/c},$$
$$C_l = 2i\Upsilon\frac{1 \pm (-1)^l}{(2\pi l \mp \phi)^2}(1 \mp e^{\pm i\phi/2}). \tag{4.47}$$

The $\pm$ modes as observed by a beam position monitor therefore contain the following frequencies:

$$\begin{aligned} &+ \text{ mode:} && \omega_\beta + l\omega_s - \frac{\phi}{2\pi}\omega_s, && l \text{ even} \\ &- \text{ mode:} && \omega_\beta + l\omega_s + \frac{\phi}{2\pi}\omega_s, && l \text{ odd.} \end{aligned} \tag{4.48}$$

Note that each mode contains a multiplicity of frequencies when observed continuously in time.

For weak beams, the two macroparticles move up and down in phase in the + mode and out of phase in the − mode. As Υ increases, the mode frequencies shift and the particle motions become more complicated; each mode then contains a combination of in-phase and out-of-phase motions. At the stability limit $\Upsilon = 2$, the frequencies of the two modes merge into each other and become imaginary, which means the beam is unstable. Figure 4.8 shows the spectrum as a function of Υ. In Figure 4.8, the index l is that appearing in Eqs. (4.47–4.48). It will also become a mode index when we consider realistic bunch distributions in Chapter 6.

If the beam receives a sudden kick at time $s/c = 0$, we have

$$\begin{bmatrix} \tilde{y}_1 \\ \tilde{y}_2 \end{bmatrix}_{s=0} = \begin{bmatrix} 1 \\ 1 \end{bmatrix}. \tag{4.49}$$

The subsequent center-of-charge motion is described as a superposition of the two eigenmodes. We find

$$(\tilde{y}_1 + \tilde{y}_2)(s) = \frac{2\Upsilon^2}{\cos(\phi/2)} e^{-i\omega_\beta s/c}\left[\exp\left(i\frac{\phi}{2\pi}\frac{\omega_s s}{c}\right)\sum_{l\,\text{even}}\frac{e^{-il\omega_s s/c}}{(2\pi l - \phi)^2}\right.$$
$$\left. - \exp\left(-i\frac{\phi}{2\pi}\frac{\omega_s s}{c}\right)\sum_{l\,\text{odd}}\frac{e^{-il\omega_s s/c}}{(2\pi l + \phi)^2}\right]. \tag{4.50}$$

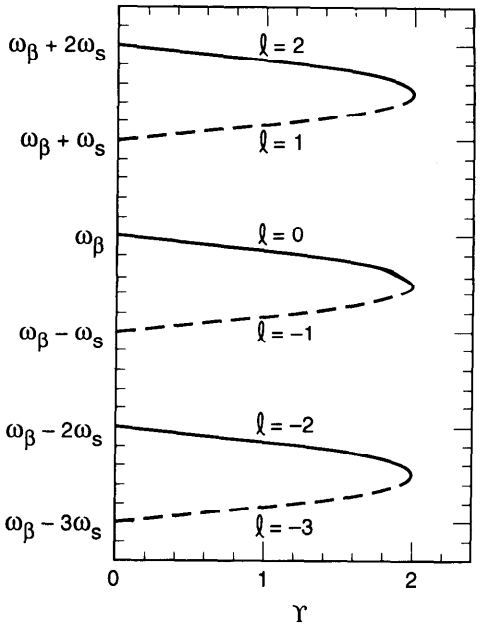

Figure 4.8. Frequency spectrum of the center-of-charge signal of the beam in the stable region $\Upsilon < 2$ in a two-particle model. The solid curves are the spectrum of the + mode, and the dashed curves are that of the − mode. Instability occurs at the point where the mode frequencies merge.

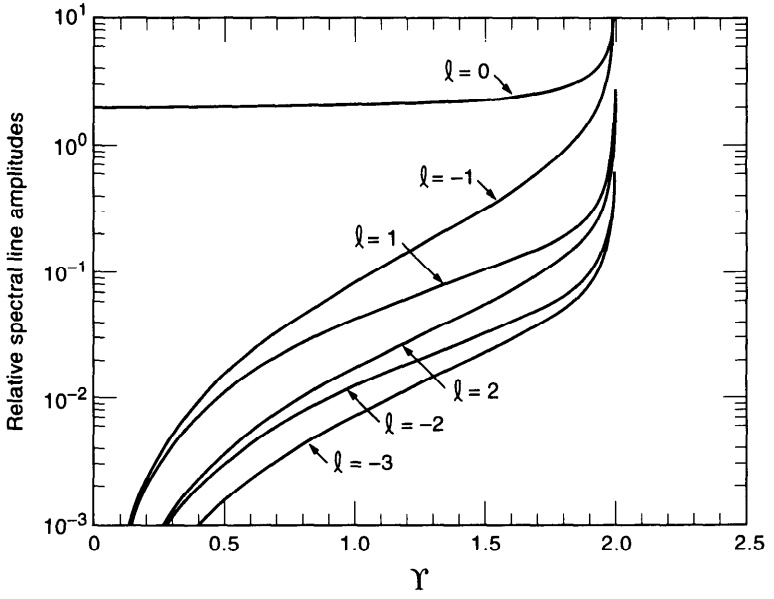

Figure 4.9. The relative amplitude of the spectral lines as observed at a beam position monitor after a two-particle beam is kicked. The spectral lines occur at frequencies given by Eq. (4.48). The normalization is arbitrarily chosen such that the $l = 0$ spectral strength at $\Upsilon = 0$ is equal to 2.

The relative amplitudes of the spectrum observed at the beam position monitor are shown in Figure 4.9 as a function of Υ. For $\Upsilon = 0$, the observed beam signal has only the unperturbed frequency ω_β. As the beam intensity increases, the amplitudes in the other spectral lines increase relative to the $l = 0$ line. Close to the instability threshold, the relative amplitudes of the $l = 0$ and the $l = -1$ lines become equal. At the threshold, all spectral line amplitudes diverge. Note that in the interest of having a high beam intensity, the accelerator is most likely operated not too far from the instability threshold.

Exercise 4.5 For modest beam intensities, one may keep only the $l = 0$ and $l = -1$ terms in Eq. (4.50). Show that the beam-position-monitor signal amplitude as a function of time exhibits a beating behavior with

$$\begin{aligned} \text{beat period} &= \frac{\pi T_s}{\pi - \phi}, \\ \text{relative depth of beat} &= \frac{2\phi^2(2\pi - \phi)^2}{\phi^4 + (2\pi - \phi)^4}. \end{aligned} \tag{4.51}$$

For weak beams, the beat frequency is the synchrotron frequency, and the depth of the beat is zero. Near the instability threshold, the beat frequency is low, while the depth for the beat approaches 100%. These expressions for the beat period and the depth of the beat can be used to extract information about the accelerator impedance from experimental measurements such as those shown in Figure 4.11 on page 186.

As mentioned, the most readily available signal from the beam is that of its center-of-charge motion observed by a beam position monitor. Using special instruments such as a streak camera, however, it is possible to observe the motion of the beam across the length of the beam. One such observation, made on the electron storage ring LEP at CERN, is shown in Figure 4.10.[19]

The strong head-tail instability is one of the cleanest instabilities to observe in electron storage rings.[20] In particular, one may measure the threshold beam intensity when the beam becomes unstable transversely and associate the observation with $\Upsilon = 2$. Another approach is to measure the "betatron frequency" (what is measured is, in fact, the frequency of the $l = 0$ spectral line of Figures 4.8 and 4.9) as the beam intensity is varied. From Eq.

[19]E. Rossa et al., *Proc. Euro. Part. Accel. Conf.*, Berlin, 1992, p. 144.

[20]R. Kohaupt, IEEE Trans. Nucl. Sci. **NS-26**, 3480 (1979); D. Rice et al., IEEE Trans. Nucl. Sci. **NS-28**, 2446 (1981); PEP Group, *Proc. 12th Int. Conf. High Energy Accel.*, Fermilab, 1983, p. 209.

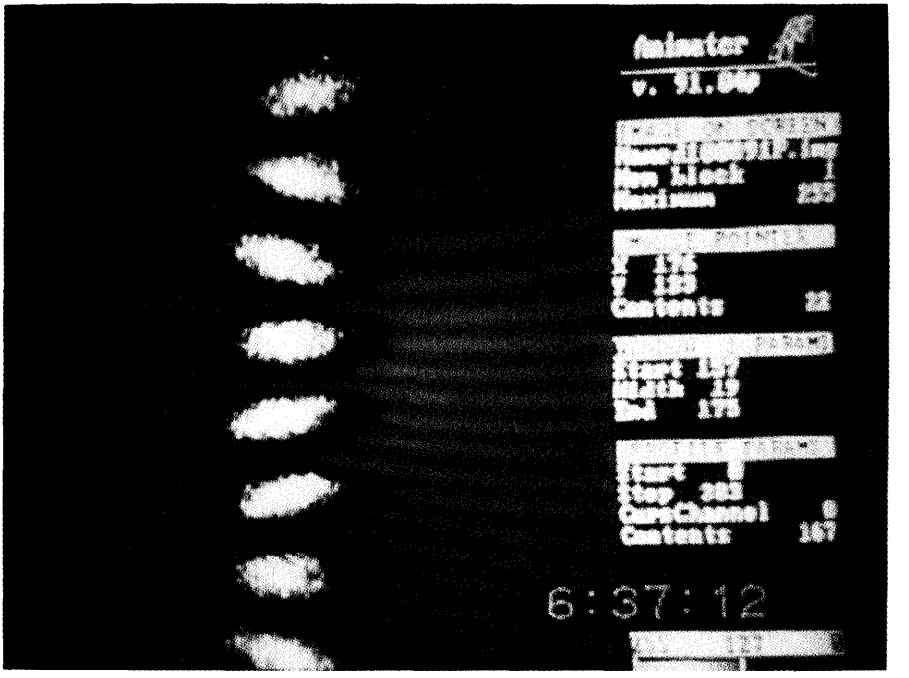

Figure 4.10. The turn-by-turn pictures, taken by a streak camera, of a beam executing a transverse head-tail oscillation in the electron storage ring LEP. The bunch is seen from the side and one observes a vertical head-tail oscillation (with mode $l = 1$). The horizontal scale is 500 ps for the total image while the vertical scale is not calibrated. The figure shows the same bunch each turn going from top to bottom. (Courtesy Albert Hofmann and Edouard Rossa, 1992.)

(4.48), the initial slope of this frequency with respect to the beam intensity is

$$\left(\frac{d\omega_\beta}{dN}\right)_{N=0} = -\frac{\omega_s}{2\pi}\left(\frac{d\phi}{dN}\right)_{N=0} = -\frac{r_0 W_0 c^2}{8\gamma C \omega_\beta}. \tag{4.52}$$

By measuring the instability threshold or by measuring the initial slope of the betatron frequency, information on the wake field or impedance can be obtained.

At the instability threshold, the measured betatron frequency has shifted by $\omega_s/2$, according to the two-particle model. The measured value of $(d\omega_\beta/dN)_{N=0}$ can be used to predict the instability threshold N_{th} by

$$N_{\text{th}} = -\frac{\omega_s}{\pi}\frac{1}{(d\omega_\beta/dN)_{N=0}}. \tag{4.53}$$

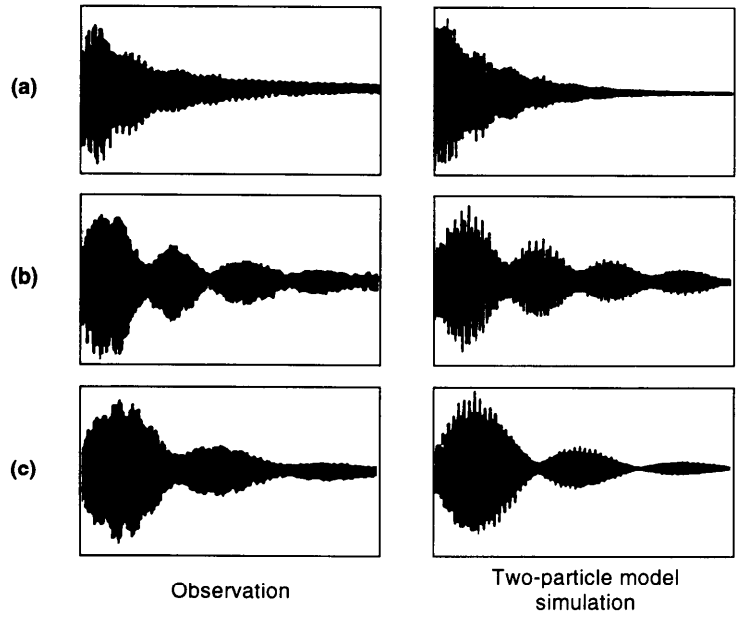

Figure 4.11. The beam-position-monitor signal as a function of time after the beam is kicked. On the left are the signals observed at the PEP storage ring: (a) is when the beam intensity N is 0.86 times the threshold intensity N_{th}, (b) $N / N_{th} = 0.93$, and (c) $N / N_{th} = 0.988$. On the right are the results of simulation using a two-particle model with (a) $\Upsilon / 2 = 0.77$, (b) $\Upsilon / 2 = 0.96$, and (c) $\Upsilon / 2 = 0.99$.

This is useful when the beam intensity is limited for reasons other than the strong head-tail instability. By measuring ω_β at low beam intensities, the eventual instability threshold can be estimated using Eq. (4.53).

Equation (4.52) indicates that the $l = 0$ frequency always shifts *down* as the beam intensity is increased. Physically, this is because, for short bunches, the sign of the wake force is such that the bunch tail is always deflected further away from the vacuum chamber axis if the beam is transversely displaced. With the head and the tail moving together in the $l = 0$ mode, the wake force acts as a defocusing effect and the mode frequency shifts down.

The center-of-charge signal of the beam as a function of time after the beam receives an initial transverse kick was analyzed in Eq. (4.50) for a two-particle model. One can also do a numerical simulation of the process. In Figure 4.11, results of the numerical simulation are compared with the experimental observation at the electron storage ring PEP.[21] Although the exact values of Υ used in the simulation have been slightly adjusted to make the comparison (see caption of Figure 4.11), the agreement is quite reasonable, indicating that the two-particle model describes this instability mecha-

[21] PEP Group, *Proc. 12th Int. Conf. High Energy Accel.*, Fermilab, 1983, p. 209.

nism remarkably well. The fact that the signal exhibits damping is due to the radiation damping effect in electron storage rings, which is not essential to the discussion here, but was included in the simulation.

The instability threshold observed at PEP occurred when the beam intensity was $N_{\text{th}} = 6.4 \times 10^{11}$ with betatron tune $\omega_\beta/\omega_0 = 18.19$, synchrotron tune $\omega_s/\omega_0 = 0.044$, $E = 14.5$ GeV, and $\omega_0 = 0.86 \times 10^6$ s^{-1}. By relating these parameters to $\Upsilon = 2$, one obtains an estimate of the wake function for PEP of $W_0 = 58$ cm^{-2}. This translates into an effective angular kick at the bunch tail of 18 μrad per millimeter of bunch head displacement per revolution. As mentioned, information on W_0 can also be obtained by measuring the betatron frequency as a function of beam intensity and applying Eq. (4.52).

These data can be used to estimate the impedances. Using Eq. (2.115), we have $Z_1^\perp \approx (R/\beta_Z \nu_\beta) b W_0/c$, where $R/\beta_Z \nu_\beta$ is the weighting factor due to β_Z, the β-function at the location of the impedance. Taking a beam pipe radius $b = 5$ cm and $R/\beta_Z \nu_\beta = 0.5$ for PEP, we find $Z_1^\perp = 0.44$ MΩ/m. Equation (2.108) then gives $Z_0^\parallel/n \approx 1.6$ Ω. This value of $Z_0^\parallel/n$ indicates that, according to Eq. (2.124), about 0.8% of the accelerator circumference is effectively occupied by cavities or their equivalents.

We have obtained the results using a two-particle beam, assuming the wake of Eq. (4.37). We will show later (see Exercise 6.25) the result of a more sophisticated calculation assuming the same wake, but taking fully into account the internal motions of the beam. We will then find that Figure 4.8 does offer a qualitative description of the beam spectrum for the $l = 0$ and $l = -1$ modes, while it is not surprising that the two-particle model fails to describe the behavior of the higher modes. It will also be shown that the instability threshold occurs when the $l = 0$ mode frequency shifts by an amount somewhat larger than, but remaining comparable to, $\omega_s/2$, the value predicted by the two-particle model.

One might want to have an idea of what happens in the unstable region. Suppose we are slightly above the instability threshold, so that $\Upsilon = 2 + \epsilon$ with $\epsilon \ll 1$. Equation (4.44) can be used to find the instability growth rate: $\tau^{-1} = 2\sqrt{\epsilon}\,/T_s$. Note the square root dependence of τ^{-1} on ϵ. This means a small ϵ can give rise to a sharp growth rate; for instance, an intensity 10% above threshold gives $\tau \approx T_s$. One consequence is that the radiation damping effect and the use of conventional feedback systems are not very effective in bringing the beam intensity substantially beyond the threshold unless the feedback damping rate is significantly larger than ω_s.

Exercise 4.6 A conventional feedback system functions by damping the center-of-charge motion of the beam. An inspection of Figure 4.8, however, suggests an alternative.[22] The instability comes about when the frequencies of modes $l = 0$ and $l = -1$ merge and become complex. By

[22] S. Myers, *Proc. IEEE Part. Accel. Conf.*, Washington, 1987, p. 503.

introducing a *reactive* feedback system—rather than the conventional system, which is resistive—that shifts the $l = 0$ mode frequency so as to delay the merging, the instability threshold may be raised. In the presence of a reactive feedback system, the equation of motion in the first half of the synchrotron period is

$$\begin{aligned} y_1'' + \left(\frac{\omega_\beta}{c}\right)^2 y_1 &= \sigma(y_1 + y_2), \\ y_2'' + \left(\frac{\omega_\beta}{c}\right)^2 y_2 &= \alpha y_1 + \sigma(y_1 + y_2), \end{aligned} \tag{4.54}$$

where $\alpha = Nr_0W_0/2\gamma C$ and σ specifies the strength of the reactive feedback, which acts on the center of charge $y_1 + y_2$ of the beam. Assuming $\omega_\beta \gg \omega_s$, show that the eigenvalues are determined by[23]

$$\lambda + \frac{1}{\lambda} = (2 - qr)\cos\mu \pm \sin\mu\sqrt{4qr - q^2r^2} \tag{4.55}$$

and stability requires $qr < 4$, where $\mu = 2\pi\omega/\omega_s$, $q = \sin^2(\pi\sigma c^2/2a\omega\omega_s)$, $\omega = \sqrt{\omega_\beta^2 - \sigma c^2}$, $r = (a + 1/a)^2$, and $a = \sqrt{\sigma/(\sigma + \alpha)}$. The instability threshold can be raised by properly choosing the feedback strength σ.

It would in principle be possible to damp the strong head-tail instability by the BNS damping introduced to prevent dipole beam breakup in linacs. The BNS condition of Eq. (3.42) for a two-particle model in a linac [or Eq. (3.48) for a general beam distribution] also gives the damping condition for a circular accelerator if $\omega_\beta \gg \omega_s$. According to Eq. (3.42), the bunch tail must be focused more strongly than the bunch head by an amount

$$\frac{\Delta\omega_\beta}{\omega_\beta} = \frac{Nr_0W_0c^2}{4\gamma C\omega_\beta^2} = \frac{\Upsilon\omega_s}{\pi\omega_\beta}, \tag{4.56}$$

where Υ is the parameter of Eq. (4.42). Near the instability threshold, $\Upsilon \approx 2$, we find $\Delta\omega_\beta/\omega_\beta = 1.5 \times 10^{-3}$ is needed to BNS damp the PEP instability mentioned above. To provide the variation of betatron focusing across the bunch, one could consider tilting the longitudinal phase space distribution of

[23]R. Ruth, CERN Report LEP-TH/83-22 (1983). In case there is an interplay among the various effects of reactive feedback, localized impedance, and synchro-betatron resonances, the picture becomes more complicated. See B. Zotter, IEEE Trans. Nucl. Sci. **NS-32**, 2191 (1985); S. Myers, CERN Report LEP-523 (1984).

the bunch so that the bunch tail has a lower energy relative to the bunch head by an amount $\Delta\delta = \Upsilon\omega_s/\pi\omega_\beta\xi$, where ξ is the chromaticity defined in Eq. (3.43). One could also consider introducing a radio frequency quadrupole magnet system.

There are some interesting effects that were inadvertently dropped when we made the approximation $\omega_\beta \gg \omega_s$ following Eq. (4.40). To recover these effects, we have to be more careful in keeping all the terms.[24] We will deal with four-dimensional vectors

$$\begin{bmatrix} y_1 \\ \dfrac{c}{\omega_\beta} y_1' \\ y_2 \\ \dfrac{c}{\omega_\beta} y_2' \end{bmatrix} \tag{4.57}$$

instead of the complex two-dimensional ones used in Eq. (4.41). The transformation for the first half of synchrotron period for this vector is found to be

$$\begin{bmatrix} A & 0 \\ B & A \end{bmatrix}, \tag{4.58}$$

where A and B are the 2×2 matrices

$$\begin{aligned} A &= \begin{bmatrix} \cos\dfrac{\mu}{2} & \sin\dfrac{\mu}{2} \\ -\sin\dfrac{\mu}{2} & \cos\dfrac{\mu}{2} \end{bmatrix}, \\ B &= \Upsilon \begin{bmatrix} \sin\dfrac{\mu}{2} & \dfrac{2}{\mu}\sin\dfrac{\mu}{2} - \cos\dfrac{\mu}{2} \\ \dfrac{2}{\mu}\sin\dfrac{\mu}{2} + \cos\dfrac{\mu}{2} & \sin\dfrac{\mu}{2} \end{bmatrix} \end{aligned} \tag{4.59}$$

with $\mu = 2\pi\omega_\beta/\omega_s$ and Υ defined in Eq. (4.42). The results obtained previously correspond to dropping terms in B that contain the factor $2/\mu$. In the second half of synchrotron period, the transformation is

$$\begin{bmatrix} A & B \\ 0 & A \end{bmatrix}. \tag{4.60}$$

[24] J. M. Jowett, CERN Report LEP-474 (1983).

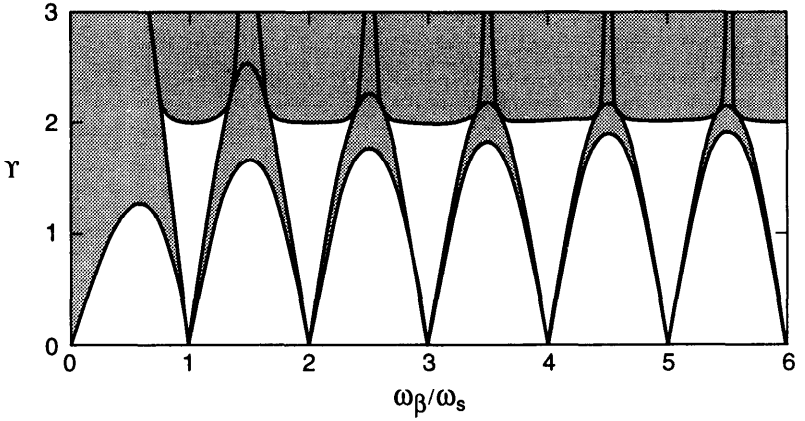

Figure 4.12. Stability region in the $(\omega_\beta / \omega_s, \Upsilon)$ plane for a two-particle beam against the strong head-tail instability. Synchro-betatron structure of the instability is pronounced near the synchro-betatron resonance conditions $\omega_\beta / \omega_s =$ integer. Unstable regions are shown shaded.

The total transformation is given by the product of the two half synchrotron periods. The resulting 4×4 matrix is then eigenanalyzed to see if the system is stable. The four eigenvalues λ are given by the roots of the characteristic function,

$$\left(\lambda + \frac{1}{\lambda}\right)^2 + 2\left(\lambda + \frac{1}{\lambda}\right)\left[\frac{2\Upsilon^2}{\mu^2}(\cos\mu - 1) + \Upsilon^2 \cos\mu - 2\cos\mu\right] + \left\{4\Upsilon^2(\cos\mu - 1) + \left[\Upsilon^2 + \frac{2\Upsilon^2}{\mu^2}(\cos\mu - 1) - 2\cos\mu\right]^2\right\} = 0. \tag{4.61}$$

Stability requires that all solutions for $\lambda + 1/\lambda$ be real and that their values be between -2 and 2.

The information we lost by assuming $\omega_\beta \gg \omega_s$ is a detailed synchro-betatron coupling effect.[25] Exercise 4.7 below shows that $\Upsilon = 2$ is the threshold condition when ω_β/ω_s is an integer or when $\omega_\beta/\omega_s \gg 1$. Away from these values of ω_β/ω_s, however, a pattern of synchro-betatron coupling emerges. The threshold value of Υ as a function of ω_β/ω_s is plotted in Figure 4.12. The synchro-betatron structure is apparent around each synchro-betatron resonance $\omega_\beta/\omega_s =$ integer, even for large values of ω_β/ω_s.

[25]Another synchro-betatron coupling mechanism, not treated here, is due to the beam having a closed-orbit distortion and a momentum dispersion at the location of the impedance. See R. Kohaupt, DESY Report 85-59 (1985); Yongho Chin, DESY Report 86-081 (1986).

Note that although the stability limit occurs at $\Upsilon = 2$ exactly on resonances $\omega_\beta = n\omega_s$, there are instability stopbands in the immediate neighborhood at low values of Υ. The regions close to the resonances are therefore to be avoided. In Figure 4.12, the stability region boundaries (the solid curves) are determined by

$$\Upsilon = \frac{2}{\sqrt{1 - \frac{4}{\mu^2}\tan^2\frac{\mu}{2}}} \quad \text{and} \quad \Upsilon = \frac{2\left|\sin\frac{\mu}{2}\right|}{1 \pm \frac{2}{\mu}\sin\frac{\mu}{2}}. \tag{4.62}$$

In case the impedance is localized at a certain position in the storage ring, the betatron frequency relevant for the resonance conditions is ω_β modulo the revolution frequency ω_0. The effective betatron frequency is then much less than ω_β itself, making the synchro-betatron structure more pronounced.

Exercise 4.7

(a) Right on a synchro-betatron resonance $\omega_\beta = n\omega_s$, use Eq. (4.61) to show that

$$\lambda + \frac{1}{\lambda} = -\Upsilon^2 + 2. \tag{4.63}$$

This gives the stability condition $\Upsilon \leq 2$.

(b) When $\omega_\beta \gg \omega_s$, show that

$$\lambda + \frac{1}{\lambda} = -(\Upsilon^2 - 2)\cos\mu \pm \Upsilon \sin\mu\sqrt{4 - \Upsilon^2}. \tag{4.64}$$

Writing $\lambda = \exp(i\mu + i\phi)$ gives Eq. (4.44). Show that the stability condition is $\Upsilon \leq 2$.

(c) When $\omega_\beta = (n + \frac{1}{2})\omega_s$, show that

$$\lambda + \frac{1}{\lambda} = -2 + \Upsilon^2\left(1 \pm \frac{2}{\mu}\right)^2 \tag{4.65}$$

and the stability condition is

$$\Upsilon \leq \frac{2\pi(n + \frac{1}{2})}{\pi(n + \frac{1}{2}) + 1}. \tag{4.66}$$

4.4 TRANSVERSE QUADRUPOLE INSTABILITY

In Chapter 3, we observed the similarity between the dipole and quadrupole beam breakup effects in linacs. In particular, we found that the perturbations at the bunch tail by the wake fields are characterized by the growth parameters from Eqs. (3.25) and (3.95) [or (3.38) and (3.96) for accelerated beams] for the dipole and quadrupole cases, respectively. For circular accelerators, we expect to find a *quadrupole strong head-tail instability* similar to the dipole strong head-tail instability discussed in the previous section. By drawing an analogy to the analysis for linacs, one is led to expect a stability condition that assumes the form

$$\Upsilon = \frac{\pi N r_0 W_0 c^2 a^2}{2\gamma C \omega_\beta \omega_s} \leq 2, \tag{4.67}$$

where a is the rms radius of the unperturbed beam cross section, and W_0 is a constant parametrizing the quadrupole wake function integrated over the accelerator circumference C, i.e.,

$$W_2(z) = -W_0 \qquad \text{for} \quad 0 > z > -(\text{bunch length}). \tag{4.68}$$

What happens here is that the throbbing motions of the bunch head and bunch tail couple through the quadrupole wake force, leading to an instability. To derive Eq. (4.67), we adopt a *two-slice* model in which the beam consists of two elliptically-shaped slices of charge $Ne/2$, each described by a symmetric 4×4 Σ-matrix whose elements are the second moments of the slice,

$$\Sigma_i = \begin{bmatrix} \langle x^2 \rangle_i & \langle xx' \rangle_i & 0 & 0 \\ \langle xx' \rangle_i & \langle x'^2 \rangle_i & 0 & 0 \\ 0 & 0 & \langle y^2 \rangle_i & \langle yy' \rangle_i \\ 0 & 0 & \langle yy' \rangle_i & \langle y'^2 \rangle_i \end{bmatrix}, \qquad i = 1, 2. \tag{4.69}$$

We have assumed the ellipses are upright in the x-y plane. The slices are assumed to execute synchrotron oscillations, and therefore exchange their leading and trailing roles every half synchrotron period $T_s/2$.

We first concentrate on the leading slice ($i = 1$). The second moments of the slice execute free betatron oscillations. The equation of motion is[26]

$$c\Sigma_1' = \Omega\Sigma_1 + \Sigma_1\tilde{\Omega}, \tag{4.70}$$

[26] Karl L. Brown, SLAC Report 75, Rev. 3 (1972).

where a tilde means taking the transpose of a matrix, and

$$\frac{\Omega}{c} = \begin{bmatrix} 0 & 1 & 0 & 0 \\ -k_x^2 & 0 & 0 & 0 \\ 0 & 0 & 0 & 1 \\ 0 & 0 & -k_y^2 & 0 \end{bmatrix} \tag{4.71}$$

with $k_{x,y}$ the betatron wave numbers. Equation (4.70) has the solution

$$\Sigma_1(s) = T\Sigma_1(0)\tilde{T}, \tag{4.72}$$

where

$$T = \begin{bmatrix} \cos k_x s & \frac{1}{k_x}\sin k_x s & 0 & 0 \\ -k_x \sin k_x s & \cos k_x s & 0 & 0 \\ 0 & 0 & \cos k_y s & \frac{1}{k_y}\sin k_y s \\ 0 & 0 & -k_y \sin k_y s & \cos k_y s \end{bmatrix}. \tag{4.73}$$

Exercise 4.8 Verify Eqs. (4.70) and (4.72) by back substitution as follows. Consider the x-dimension only. We know the single-particle motion has the solution

$$\begin{aligned} x(s) &= x_0 \cos k_x s + \frac{x_0'}{k_x}\sin k_x s \\ x'(s) &= -k_x x_0 \sin k_x s + x_0' \cos k_x s. \end{aligned} \tag{4.74}$$

It follows that

$$\begin{aligned} \langle x^2\rangle(s) &= \langle x^2\rangle_0 \cos^2 k_x s + \frac{\langle xx'\rangle_0}{k_x}\sin 2k_x s + \frac{\langle x'^2\rangle_0}{k_x^2}\sin^2 k_x s, \\ \langle xx'\rangle(s) &= -\frac{k_x\langle x^2\rangle_0}{2}\sin 2k_x s + \langle xx'\rangle_0 \cos 2k_x s + \frac{\langle x'^2\rangle_0}{2k_x}\sin 2k_x s, \\ \langle x'^2\rangle(s) &= k_x^2\langle x^2\rangle_0 \sin^2 k_x s - k_x\langle xx'\rangle_0 \sin 2k_x s + \langle x'^2\rangle_0 \cos^2 k_x s, \end{aligned} \tag{4.75}$$

which can be shown to satisfy Eqs. (4.70) and (4.72). Also show that the quantity

$$\det(\Sigma_x) = \langle x^2\rangle\langle x'^2\rangle - \langle xx'\rangle^2 \tag{4.76}$$

is a constant of the motion. This quantity is related to the beam emittance according to Eq. (1.94).

In the following we will do a perturbation calculation. Let

$$\begin{aligned}
\langle x^2\rangle_i &= a^2 + A_{xi},\\
\langle xx'\rangle_i &= 0 + B_{xi},\\
\langle x'^2\rangle_i &= k_x^2 a^2 + C_{xi},\\
\langle y^2\rangle_i &= a^2 + A_{yi},\\
\langle yy'\rangle_i &= 0 + B_{yi},\\
\langle y'^2\rangle_i &= k_y^2 a^2 + C_{yi}, \qquad i = 1,2
\end{aligned} \tag{4.77}$$

The first terms on the right hand sides are the unperturbed values, and the second terms are small, time dependent perturbations. We have assumed that the unperturbed beam is round with rms radius a. The index i refers to the two slices.

Since the beam emittances

$$\sqrt{\langle x^2\rangle_i\langle x'^2\rangle_i - \langle xx'\rangle_i^2} \quad \text{and} \quad \sqrt{\langle y^2\rangle_i\langle y'^2\rangle_i - \langle yy'\rangle_i^2}$$

are constants of the motion, it follows that $k_x^2 A_{xi} + C_{xi}$ and $k_y^2 A_{yi} + C_{yi}$ are invariants. Without losing any beam stability information, we are therefore free to choose the constraints

$$\begin{aligned}
C_{xi} &= -k_x^2 A_{xi},\\
C_{yi} &= -k_y^2 A_{yi}, \qquad i = 1,2.
\end{aligned} \tag{4.78}$$

In terms of the perturbation moments, Eq. (4.72) or (4.75) can be written explicitly as

$$\begin{aligned} A_{x1}(s) &= A_{x1}(0)\cos 2k_x s + \frac{1}{k_x}B_{x1}(0)\sin 2k_x s, \\ B_{x1}(s) &= -k_x A_{x1}(0)\sin 2k_x s + B_{x1}(0)\cos 2k_x s, \end{aligned} \tag{4.79}$$

and another set of expressions with x replaced by y. Equation (4.79) describes the free quadrupole oscillation of the first slice. The oscillation frequency of its second moments is twice the free betatron oscillation.

Bunch slice 1 leaves behind a quadrupole wake force that, according to Eq. (3.82), is equivalent to the force due to a quadrupole magnet with a gradient $\partial B_y/\partial x = -NeW_0(\langle x^2\rangle_1 - \langle y^2\rangle_1)/C = -NeW_0(A_{x1} - A_{y1})/C$. The equation of motion of the trailing slice can be obtained by modifying the betatron focusing according to

$$\begin{aligned} k_x^2 &\to k_x^2 - \frac{Nr_0W_0}{\gamma C}(A_{x1} - A_{y1}), \\ k_y^2 &\to k_y^2 + \frac{Nr_0W_0}{\gamma C}(A_{x1} - A_{y1}). \end{aligned} \tag{4.80}$$

To first order in the perturbations A_{xi}, B_{xi}, A_{yi}, and B_{yi}, we then have

$$c\Sigma_2' = \Omega\Sigma_2 + \Sigma_2\tilde{\Omega} + \frac{Nr_0W_0ca^2}{\gamma C}(A_{x1} - A_{y1})\begin{bmatrix} 0 & 1 & 0 & 0 \\ 1 & 0 & 0 & 0 \\ 0 & 0 & 0 & -1 \\ 0 & 0 & -1 & 0 \end{bmatrix}, \tag{4.81}$$

where the matrix Ω is that defined in Eq. (4.71). Equation (4.81) can be integrated exactly, but we will keep only the resonant terms. We assume k_x and k_y are different, so that there is no resonant coupling between the two dimensions, and we need only to consider one of the two dimensions, say the x-dimension. Substituting Eq. (4.79) into Eq. (4.81) then yields, after some algebraic manipulations,

$$\Sigma_2(s) = TS\tilde{T}, \tag{4.82}$$

where T is the 2×2 block of Eq. (4.73) and

$$S = \Sigma_2(0) + \frac{Nr_0W_0a^2s}{2\gamma C}\begin{bmatrix} -\frac{1}{k_x^2}B_1(0) & A_1(0) \\ A_1(0) & B_1(0) \end{bmatrix}. \tag{4.83}$$

We have dropped the subscript x from all the A's and B's. Note that the second term in S is proportional to s.

The solution (4.82–4.83), written in terms of the perturbation moments, gives

$$\begin{aligned} A_2(s) &= A_2(0)\cos 2k_x s + \frac{B_2(0)}{k_x}\sin 2k_x s \\ &\quad + \frac{Nr_0W_0a^2s}{2\gamma Ck_x}\left[-\frac{B_1(0)}{k_x}\cos 2k_x s + A_1(0)\sin 2k_x s\right], \\ B_2(s) &= -k_x A_2(0)\sin 2k_x s + B_2(0)\cos 2k_x s \\ &\quad + \frac{Nr_0W_0a^2s}{2\gamma C}\left[\frac{B_1(0)}{k_x}\sin 2k_x s + A_1(0)\cos 2k_x s\right]. \end{aligned} \tag{4.84}$$

Equation (4.84) is the solution during the time $0 < s/c < T_s/2$. If we now form two phasors

$$\begin{aligned} \tilde{Q}_1 &= A_1 + i\frac{B_1}{k_x}, \\ \tilde{Q}_2 &= A_2 + i\frac{B_2}{k_x}, \end{aligned} \tag{4.85}$$

the transformation from $s = 0$ to $s = cT_s/2$ is found to be

$$\begin{bmatrix} \tilde{Q}_1 \\ \tilde{Q}_2 \end{bmatrix}_{s=cT_s/2} = e^{-ik_x cT_s}\begin{bmatrix} 1 & 0 \\ i\Upsilon & 1 \end{bmatrix}\begin{bmatrix} \tilde{Q}_1 \\ \tilde{Q}_2 \end{bmatrix}_0, \tag{4.86}$$

where Υ is the parameter defined in Eq. (4.67).

Equation (4.86) appears almost identical to its dipole counterpart, Eq. (4.41). The same analysis of the previous section then leads to the expected stability criterion (4.67). The frequency spectrum of the two-slice beam under the influence of a quadrupole wake therefore looks the same as Figure 4.8, except that the mode frequencies cluster around $2\omega_\beta$ instead of ω_β.

The ratio of the quadrupole strength parameter (4.67) to the dipole parameter (4.42) is of the order of $2a^2/b^2$, where a is the rms transverse beam size, and b is the size of the vacuum chamber where the impedance is

located. Quadrupole instability is relatively unimportant unless the beam virtually fills the vacuum chamber.

4.5 HEAD-TAIL INSTABILITY

In our analysis of the strong head-tail instability in Section 4.3, we assumed that the betatron and the synchrotron motions are decoupled from each other. In doing so, we ignored an important source of instability known as the *head-tail instability*, to which we now turn.

The head-tail instability is one of the cleanest to be observed experimentally.[27] Although it involves a mechanism more subtle than that of the strong head-tail instability, this instability can occur at much lower beam intensities. This may explain the fact that it was actually observed and explained[28] earlier than the strong head-tail instability.[29]

The betatron oscillation frequency of a particle in a circular accelerator depends on the energy error $\delta = \Delta E/E$ of the particle. If we denote that betatron frequency of an on-momentum particle as ω_β, the betatron frequency for an off-momentum particle can be written as

$$\omega_\beta(\delta) = \omega_\beta(1 + \xi\delta), \tag{4.87}$$

where ξ is the chromaticity parameter determined by the accelerator design and was introduced already in Eq. (3.43).[30] To assure that the beam has a small betatron frequency spread due to a spread in δ, the absolute value of ξ must not be too large. A consequence of the head-tail consideration, as we will soon see, is that in addition to this requirement, ξ must also have a definite sign. The main reason for introducing sextupoles in circular accelerators is, in fact, to control ξ.

In Section 4.3, we have used s, the longitudinal coordinate along the accelerator, as the independent variable, and the time t is related to s simply by $s = ct$. It is no longer so simple here, because now we have to consider synchrotron motions, and the varying time of arrival confounds the connection between s and t. It turns out to be simpler to use s as the independent variable, as will be done below.

[27]The SPEAR Group, *Proc. 9th Int. Conf. High Energy Accel.*, SLAC, 1974, p. 338; J. Gareyte and F. Sacherer, *Proc. 9th Int. Conf. High Energy Accel.*, SLAC, 1974, p. 341; Y. Miyahara and K. Takata, Part. Accel. **10**, 125 (1980).

[28]C. Pellegrini, Nuovo Cimento **64A**, 447 (1969); M. Sands, SLAC Reports TN-69-8 and TN-69-10 (1969). See also F. Sacherer, CERN Report SI-BR/72-5 (1972); F. Sacherer, *Proc. 9th Int. Conf. High Energy Accel.*, SLAC, 1974, p. 347.

[29]It may also explain the fact that this instability has preempted the name of "head-tail instability" although almost any other collective instability could justify the same name.

[30]Sometimes in the literature the chromaticity is defined differently, as $\omega_\beta(\delta) = \omega_\beta + \xi\delta\omega_0$.

Let us first examine the free betatron oscillation in the absence of wake fields. The accumulated betatron phase is given by an integration of Eq. (4.87), i.e.,

$$\phi_\beta(s) = \int \omega_\beta(\delta)\frac{ds}{c} = \omega_\beta\left(\frac{s}{c} + \xi\int\delta\frac{ds}{c}\right)$$
$$= \omega_\beta\left[\frac{s}{c} - \frac{\xi}{c\eta}z(s)\right], \tag{4.88}$$

where η is the slippage factor, and we have used Eq. (1.9), $z' = -\eta\delta$.

Equation (4.88) is already a remarkable result. It says that the deviation of the betatron phase of a particle from the nominal value $\omega_\beta s/c$ is determined by its longitudinal position. In other words, the chromatic modulation of the betatron phase depends only on z and not on other dynamic variables, such as δ.[31] The modulation, of course, is slow and weak.

We now consider two macroparticles whose synchrotron oscillations are given by

$$z_1 = \hat{z}\sin\frac{\omega_s s}{c} \quad \text{and} \quad z_2 = -z_1, \tag{4.89}$$

where ω_s is the synchrotron oscillation frequency. Particle 1 leads particle 2 during $0 < s/c < \pi/\omega_s$ and trails it during $\pi/\omega_s < s/c < 2\pi/\omega_s$. The free betatron oscillations of the two particles are described by

$$y_1(s) = \tilde{y}_1 e^{-i\phi_{\beta 1}(s)} = \tilde{y}_1 \exp\left(-i\omega_\beta\frac{s}{c} + i\frac{\xi\omega_\beta}{c\eta}\hat{z}\sin\frac{\omega_s s}{c}\right),$$
$$y_2(s) = \tilde{y}_2 e^{-i\phi_{\beta 2}(s)} = \tilde{y}_2 \exp\left(-i\omega_\beta\frac{s}{c} - i\frac{\xi\omega_\beta}{c\eta}\hat{z}\sin\frac{\omega_s s}{c}\right). \tag{4.90}$$

As the particles exchange the roles of leading particle and trailing particle, the betatron phases are such that the leading particle always lags in phase relative to the trailing particle if $\xi/\eta > 0$ and the situation reverses if $\xi/\eta < 0$, as illustrated in Figure 4.13.

The factor $\xi\omega_\beta\hat{z}/c\eta$ is called the *head-tail phase*. It is the physical origin of the head-tail instability. As a numerical example, one may have an electron accelerator with $\eta = 0.003$, $\xi = 0.2$, $\hat{z} = 3$ cm, and $\omega_\beta = 1.4 \times 10^7\ \text{s}^{-1}$, which gives a head-tail phase of $2\pi \times 0.016$.

Recalling the strong head-tail instability studied previously, the trailing particle is always unstable due to the resonant driving by the wake field of

[31] Modulation of the betatron phase by z or the betatron frequency by δ leads to an instability. Modulation of the betatron phase by δ or the betatron frequency by z does not lead to an instability.

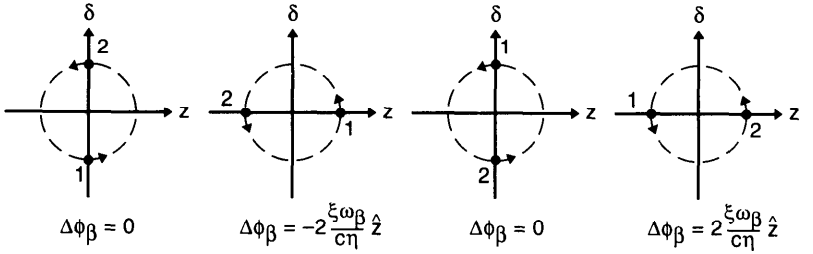

Figure 4.13. The synchrotron oscillation of a two-particle beam observed in the longitudinal phase space. The quantity $\Delta\phi_\beta = \phi_{\beta 1} - \phi_{\beta 2}$ is the difference of the betatron phases of the two particles; it is modulated by the synchrotron motion as shown. The sense of rotation of particle motion in the phase space is for the case above transition, i.e., $\eta > 0$.

the leading particle; the growths of the trailing particle during the half synchrotron periods are strong, but below a certain threshold the synchrotron oscillation washes away the growths and the net result is that the beam becomes stable. The additional chromatic term that we are considering now does not have this fortunate property. As we will see, the weak growths associated with chromaticity do accumulate persistently from one half synchrotron period to the next, and thus slowly build up an instability without a threshold.

Let us look at the motion of particle 2 during $0 < s/c < \pi/\omega_s$ in the presence of the wake field. The wake function, we assume, is that given by Eq. (4.37). The equation of motion is

$$y_2'' + \left[\frac{\omega_\beta(\delta_2)}{c}\right]^2 y_2 = \frac{Nr_0W_0}{2\gamma C} y_1,$$
$$\omega_\beta(\delta_2) = \omega_\beta\left(1 + \frac{\xi\hat{z}\omega_s}{c\eta}\cos\frac{\omega_s s}{c}\right). \tag{4.91}$$

The y_1 on the right hand side is given by the free oscillation result from Eq. (4.90). If we let y_2 also be given by Eq. (4.90), but allow $\tilde{y}_2$ to be slowly varying in time, Eq. (4.91) leads to an equation for $\tilde{y}_2$,

$$\tilde{y}_2'(s) \approx \frac{iNr_0W_0c}{4\gamma C\omega_\beta}\tilde{y}_1(0)\exp\left(2i\frac{\xi\omega_\beta\hat{z}}{c\eta}\sin\frac{\omega_s s}{c}\right). \tag{4.92}$$

For most practical cases, the head-tail phase $\xi\omega_\beta\hat{z}/c\eta$ is much less than unity, the exponential factor in Eq. (4.92) can be Taylor expanded, and y_2

can be integrated to yield

$$\tilde{y}_2(s) = \tilde{y}_2(0) + \frac{iNr_0W_0c}{4\gamma C\omega_\beta}\tilde{y}_1(0)\left[s + i\frac{2\xi\omega_\beta\hat{z}}{\eta\omega_s}\left(1 - \cos\frac{\omega_s s}{c}\right)\right]. \quad (4.93)$$

The first term in the brackets is the resonant response already studied in Section 4.3 and is responsible for the strong head-tail instability. The second, chromatic term is small, because it is proportional to the head-tail phase and also because it is not a resonant response. On the other hand, the important fact here is that the chromatic term is 90° out of phase from the resonant term.

The transformation from $s = 0$ to $s = \pi c/\omega_s$ is thus described by

$$\begin{bmatrix}\tilde{y}_1\\ \tilde{y}_2\end{bmatrix}_{\pi c/\omega_s} = \begin{bmatrix}1 & 0\\ i\Upsilon & 1\end{bmatrix}\begin{bmatrix}\tilde{y}_1\\ \tilde{y}_2\end{bmatrix}_0, \quad (4.94)$$

where

$$\Upsilon = \frac{\pi Nr_0W_0c^2}{4\gamma C\omega_\beta\omega_s}\left(1 + i\frac{4\xi\omega_\beta\hat{z}}{\pi c\eta}\right). \quad (4.95)$$

This Υ, of course, reduces to Eq. (4.42) if $\xi = 0$, but now it has acquired an imaginary part if $\xi \neq 0$. A similar procedure applied to the period $\pi c/\omega_s < s < 2\pi c/\omega_s$ leads to the transformation

$$\begin{bmatrix}\tilde{y}_1\\ \tilde{y}_2\end{bmatrix}_{2\pi c/\omega_s} = \begin{bmatrix}1 & i\Upsilon\\ 0 & 1\end{bmatrix}\begin{bmatrix}\tilde{y}_1\\ \tilde{y}_2\end{bmatrix}_{\pi c/\omega_s}. \quad (4.96)$$

As we did before, the stability of the system is determined by the total transformation matrix

$$\begin{bmatrix}1 & i\Upsilon\\ 0 & 1\end{bmatrix}\begin{bmatrix}1 & 0\\ i\Upsilon & 1\end{bmatrix} = \begin{bmatrix}1 - \Upsilon^2 & i\Upsilon\\ i\Upsilon & 1\end{bmatrix}. \quad (4.97)$$

The eigenvalues of this matrix have been obtained before in Eq. (4.44). For a weak beam intensity, $|\Upsilon| \ll 1$, the two eigenvalues are

$$\lambda_\pm \approx e^{\pm i\Upsilon}. \quad (4.98)$$

The + mode (− mode) is the mode when the two macroparticles oscillate in phase (out of phase) in the limit of weak beam intensity. The imaginary part

of Υ thus gives a growth rate of the betatron oscillations,

$$\tau_{\pm}^{-1} = \mp \frac{Nr_0 W_0 c\xi\hat{z}}{2\pi\gamma C\eta}. \tag{4.99}$$

When the + mode is unstable, the − mode is stable; the transverse displacement of the beam center of charge grows with time, but the transverse size of the beam essentially remains constant. When the − mode is unstable, the + mode becomes stable; the beam center of charge does not oscillate, but the beam size grows exponentially.

The + mode is damped if $\xi/\eta > 0$ and antidamped if $\xi/\eta < 0$. The − mode is damped if $\xi/\eta < 0$ and antidamped if $\xi/\eta > 0$. We conclude from this that the only value of ξ that assures a stable beam is $\xi = 0$. However, as we will see later in Chapter 6 using a Vlasov equation technique, the two-particle model has overestimated the growth rate of the − mode. This consideration, together with the presence of some stabilizing mechanisms (such as Landau damping, or radiation damping in the case of circular electron accelerators) leads us to choose slightly positive values for ξ for operation above transition, and slightly negative ξ below transition.

The growth rate is proportional to N and ξ, and inversely proportional to γ as one would expect. The linear dependence on the bunch length $\hat{z}$ as given in Eq. (4.99), however, is a consequence of the constant wake model. Had we assumed a different wake model, the dependence of τ^{-1} on $\hat{z}$ would change. Another examination of the structure of Eq. (4.99) will be given later in Eqs. (6.219–6.220).

Note that the same transverse wake field is responsible for the strong head-tail instability and the head-tail instability. Continuing the PEP example mentioned after Eq. (4.53), and further taking $\hat{z} = 3$ cm and $\xi = 0.2$, we find the head-tail growth rate ∓ 0.6 ms at the threshold for strong head-tail instability, $N = 6.4 \times 10^{11}$.[32] The head-tail damping or antidamping can be rather fast.

In addition to the methods mentioned after Eq. (4.53), the head-tail growth rate provides another way to measure the transverse wake function and the impedance of an accelerator. To do so, ξ is made slightly positive (above transition), a beam center-of-charge motion (in a + mode) is excited by a kicker, and its subsequent damped motion is observed. The linear dependence of the damping rate on ξ allows the extraction of the wake function information. The various methods of measuring the wake function are not expected to give identical values for the transverse impedance $Z_1^{\perp}$, but the results should at least be comparable.

[32]Strictly speaking, Eq. (4.99) applies only when $|\Upsilon| \ll 1$. We apply it here, even though $\mathrm{Re}\,\Upsilon = 2$, to obtain an order of magnitude estimate.

Once $Z_1^\perp$ is established, Eq. (2.108) gives an estimate of $Z_0^\parallel/n$. One may compare the value of $Z_0^\parallel/n$ obtained this way with that obtained by measuring the parasitic loss, which was discussed following Eq. (2.201).

Exercise 4.9 In case the head-tail phase is not much less than unity, show that the parameter Υ is given by

$$\Upsilon = \frac{Nr_0W_0c^2}{4\gamma C\omega_\beta\omega_s} f\left(\frac{2\xi\omega_\beta\hat{z}}{c\eta}\right), \qquad f(u) = \int_0^\pi dx\, e^{iu\sin x}. \tag{4.100}$$

The function $f(u)$ is plotted in Figure 4.14. The real part of $f(u)$ is equal to π times the Bessel function $J_0(u)$. Since the real part of Υ is responsible for the strong head-tail instability, and the imaginary part of Υ is responsible for the head-tail instability, Eq. (4.100) indicates that it is in principle possible to increase the strong head-tail threshold by having a head-tail phase so that $u \approx 2.405$, the root of $J_0(u)$. The imaginary part of f can be used to obtain the head-tail growth rates

$$\tau_\pm^{-1} = \mp \frac{Nr_0W_0c^2}{8\pi\gamma C\omega_\beta} \operatorname{Im} f\left(\frac{2\xi\omega_\beta\hat{z}}{c\eta}\right). \tag{4.101}$$

In particular, $\tau_\pm^{-1} = 0$ if $u = 0$ or $u = 4.33$.

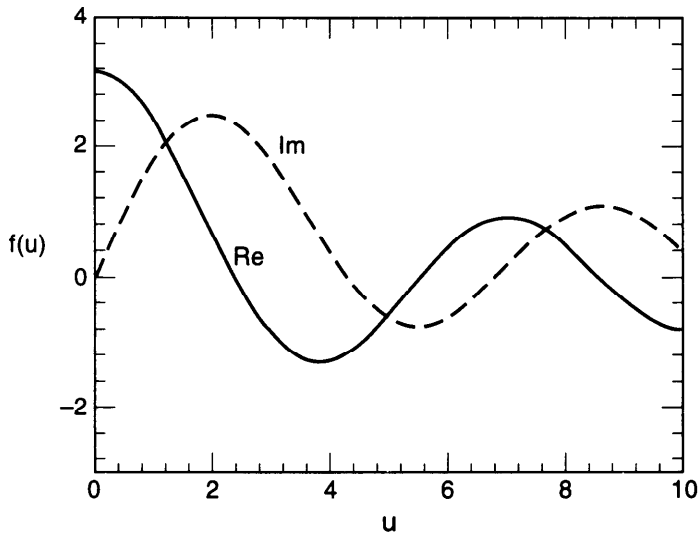

Figure 4.14. The function $f(u)$ in Eq. (4.100).

Exercise 4.10 It was observed in the electron storage ring SPEAR I that the head-tail damping time is 1 ms under the conditions $I = 20$ mA, $E = 1.5$ GeV, $\xi = 0.67$, $\hat{z} = 13$ cm, $\eta = 0.037$, $C = 240$ m, $b = 5$ cm.[33] Estimate the magnitudes of the transverse wake function and the impedances $Z_1^{\perp}$ and $Z_0^{\parallel}/n$.

Exercise 4.11 Suppose the linear chromaticity ξ has been accurately made to vanish, the leading chromatic term is therefore quadratic in δ, i.e., $\omega_\beta(\delta) = \omega_\beta(1 + \xi_2\delta^2)$. Does such an accelerator have a head-tail instability? First consider a constant wake, then a general wake.

4.6 MULTIPLE BUNCHES

So far we have treated a beam that has only one bunch of particles. In this section, we will consider a beam with multiple bunches. To be specific, consider first a beam that has two bunches circulating in the same direction in the accelerator. Let each bunch be a point charge Ne, and let the two bunches be separated by half the accelerator circumference. We will specify the two bunches by indices 0 and 1.

We assume that a transverse $m = 1$ wake force is functioning. The equations of motion for the two point macroparticles are

$$\ddot{y}_0(t) + \omega_\beta^2 y_0(t) = -\frac{Nr_0c}{\gamma T_0}\sum_{k=0}^{\infty}\left[W_1\left(-kC - \frac{C}{2}\right)y_1\left(t - kT_0 - \frac{T_0}{2}\right) + W_1(-kC)\,y_0(t - kT_0)\right], \tag{4.102}$$

and another equation with y_0 and y_1 exchanged, where $C = cT_0$ is the accelerator circumference. The index k sums over all previous revolutions. We have used time t as the independent variable.

Let the two bunches be executing transverse motion in a mode with frequency Ω, i.e.,

$$y_{0,1}(t) = \tilde{y}_{0,1}e^{-i\Omega t}. \tag{4.103}$$

The complex quantities $\tilde{y}_{0,1}$ give the amplitudes and phases at a fixed time t, i.e., they are the "snapshot" quantities rather than quantities observed at a fixed location.

[33]The SPEAR Group, *9th Int. Conf. on High Energy Accel.*, Stanford, 1974, p. 338.

Substituting Eq. (4.103) into Eq. (4.102) and assuming Ω is close to ω_β, we obtain

$$\begin{aligned}(\Omega - \omega_\beta + \omega_\beta \Upsilon_A)\tilde{y}_0 + \omega_\beta \Upsilon_B \tilde{y}_1 &= 0,\\ \omega_\beta \Upsilon_B \tilde{y}_0 + (\Omega - \omega_\beta + \omega_\beta \Upsilon_A)\tilde{y}_1 &= 0,\end{aligned} \tag{4.104}$$

where we have introduced two dimensionless quantities

$$\begin{aligned}\Upsilon_A &= -\frac{Nr_0 c}{2\gamma T_0 \omega_\beta^2} \sum_{k=0}^{\infty} W_1(-kC) e^{i\omega_\beta k T_0},\\ \Upsilon_B &= -\frac{Nr_0 c}{2\gamma T_0 \omega_\beta^2} \sum_{k=0}^{\infty} W_1\left(-kC - \frac{C}{2}\right) e^{i\omega_\beta (k+1/2) T_0}.\end{aligned} \tag{4.105}$$

In terms of the impedance, Eq. (4.105) reads

$$\begin{aligned}\Upsilon_A &= i\frac{Nr_0 c}{2\gamma T_0^2 \omega_\beta^2} \sum_{p=-\infty}^{\infty} Z_1^{\perp}(p\omega_0 + \omega_\beta),\\ \Upsilon_B &= i\frac{Nr_0 c}{2\gamma T_0^2 \omega_\beta^2} \sum_{p=-\infty}^{\infty} (-1)^p Z_1^{\perp}(p\omega_0 + \omega_\beta),\end{aligned} \tag{4.106}$$

where $\omega_0 = 2\pi/T_0$.

The only solution to the pair of equations (4.104) is the trivial solution $\tilde{y}_0 = \tilde{y}_1 = 0$, unless

$$\det\begin{bmatrix} \Omega - \omega_\beta + \omega_\beta \Upsilon_A & \omega_\beta \Upsilon_B \\ \omega_\beta \Upsilon_B & \Omega - \omega_\beta + \omega_\beta \Upsilon_A \end{bmatrix} = 0. \tag{4.107}$$

In other words, in order for a mode to exist, Ω must satisfy Eq. (4.107). Solving it gives two values for Ω,

$$\begin{aligned}\Omega_{\pm} - \omega_\beta &= -\omega_\beta(\Upsilon_A \pm \Upsilon_B)\\ &= -i\frac{Nr_0 c}{2\gamma T_0^2 \omega_\beta} \sum_{p=-\infty}^{\infty} \left[1 \pm (-1)^p\right] Z_1^{\perp}(p\omega_0 + \omega_\beta).\end{aligned} \tag{4.108}$$

It follows that the + mode is affected only by the impedance sampled at $p\omega_0 + \omega_\beta$ with even p's, while the − mode is affected only by odd p's. Compared with Eqs. (4.27–4.28) for the single-bunch case, the right hand side of Eq. (4.108) contains an extra factor of two, but the summation over p is twice as sparse. Note that N is the number of particles per bunch, not the total number of particles in the beam.

Substituting Eq. (4.108) into Eq. (4.104), we find that the snapshot displacements of the two bunches oscillate in phase for the + mode and out of phase for the − mode, i.e.,

$$\begin{aligned} \tilde{y}_0 &= \tilde{y}_1 \qquad \text{for + mode,} \\ \tilde{y}_0 &= -\tilde{y}_1 \qquad \text{for − mode.} \end{aligned} \tag{4.109}$$

For this reason, the + mode is also called the 0-mode and the − mode is called the π-mode. The fact that the two eigenmodes of the two bunches have the simple pattern (4.109) is independent of the strength of the coupling (i.e., the beam intensity and the impedance) between them.

The above analysis can be generalized to the case of M equally spaced, equally populated bunches. Let $y_n(t)$ $(n = 0, 1, \ldots, M-1)$ be the snapshot displacements of the individual bunches. The indexing is such that the $n = 1$ bunch is ahead of the $n = 0$ bunch, the $n = 2$ bunch is ahead of the $n = 1$ bunch, etc. The equations of motion are

$$\begin{aligned} \ddot{y}_n(t) + \omega_\beta^2 y_n(t) = &-\frac{Nr_0 c}{\gamma T_0} \sum_k \sum_{m=0}^{M-1} W_1\left(-kC - \frac{m-n}{M}C\right) \\ &\times y_m\left(t - kT_0 - \frac{m-n}{M}T_0\right). \end{aligned} \tag{4.110}$$

Letting

$$y_n(t) = \tilde{y}_n e^{-i\Omega t}, \tag{4.111}$$

we obtain

$$\begin{aligned} (\Omega - \omega_\beta)\tilde{y}_n &= \frac{Nr_0 c}{2\gamma T_0 \omega_\beta} \sum_{m=0}^{M-1} \tilde{y}_m \sum_k \exp\left[i\omega_\beta T_0\left(k + \frac{m-n}{M}\right)\right] \\ &\quad \times W_1\left(-kC - \frac{m-n}{M}C\right) \\ &= -i\frac{Nr_0 c}{2\gamma T_0^2 \omega_\beta} \sum_{m=0}^{M-1} \tilde{y}_m \sum_p Z_1^\perp(p\omega_0 + \omega_\beta)\exp\left(-i2\pi p\frac{m-n}{M}\right). \end{aligned} \tag{4.112}$$

There will be a total of M modes of the multibunch motion, each specified by an index μ which assumes the values $0, 1, \ldots, M-1$. The amplitudes of the M bunches, as the whole beam is executing the μth multibunch mode, are given by

$$\tilde{y}_n^{(\mu)} \propto e^{2\pi i \mu n/M}. \tag{4.113}$$

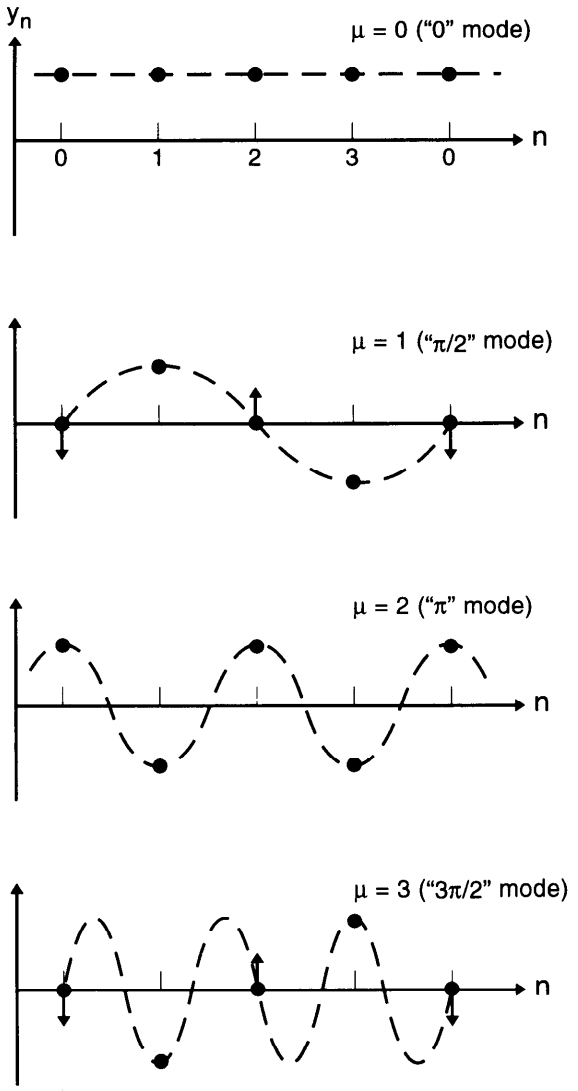

Figure 4.15. Snapshot patterns of the multibunch modes for a beam with four bunches. Arrows indicate the instantaneous directions of motion of a bunch.

The oscillation amplitudes y_n in various modes are shown in Figure 4.15 for the case of $M = 4$. The mode frequencies, obtained by substituting Eq. (4.113) into Eq. (4.112), are given by

$$\Omega^{(\mu)} - \omega_\beta = -i\frac{MNr_0c}{2\gamma T_0^2\omega_\beta}\sum_{p=-\infty}^{\infty} Z_1^\perp\left[\omega_\beta + (pM + \mu)\omega_0\right]. \quad (4.114)$$

For $M = 2$, Eq. (4.114) reduces to Eq. (4.108) if we identify $\mu = 0$ with the + mode and $\mu = 1$ with the − mode.

Compared with Eq. (4.25), these complex mode frequency shifts contain an extra factor of M in front, but the summation is M times as sparse. For an impedance broader than $M\omega_0$, Eq. (4.114) gives the same result as Eq. (4.25). This is expected, because in this case the wake field is shorter than the spacing between bunches and the beam behaves as M individual bunches which do not interact with one another. For sharp impedances, however, the difference between Eq. (4.114) and Eq. (4.25) can be substantial.

The reason the impedance is evaluated at $\omega = \omega_\beta + pM\omega_0 + \mu\omega_0$ can be understood similarly as Eq. (4.30). Observed at a fixed location where the impedance is located, the signal from a beam executing the μth multibunch mode is

$$\text{beam signal} \propto \sum_{k=-\infty}^{\infty} \sum_{n=0}^{M-1} y_n^{(\mu)}(t)\,\delta\left(t - kT_0 + \frac{nT_0}{M}\right)$$

$$\propto \sum_k \sum_n e^{-i\omega_\beta t} e^{i2\pi\mu n/M} \delta\left(t - kT_0 + \frac{nT_0}{M}\right). \qquad (4.115)$$

The spectrum of this signal is

$$\text{spectrum} \propto \int dt\, e^{i\omega t}(\text{beam signal})$$

$$\propto \sum_k \sum_n e^{i2\pi\mu n/M} \exp\left[i(\omega - \omega_\beta)\left(kT_0 - \frac{nT_0}{M}\right)\right]$$

$$= M\omega_0 \sum_{p=-\infty}^{\infty} \delta(\omega - \omega_\beta - pM\omega_0 - \mu\omega_0). \qquad (4.116)$$

The μth multibunch mode therefore samples the betatron sidebands of the frequencies $(pM + \mu)\omega_0$ where $p = \pm$ integers, as Eq. (4.114) indicates.

As an application of Eq. (4.114), consider a resistive wall. Recall that, with a $\omega^{-1/2}$ dependence, the transverse resistive-wall impedance is large at low frequencies. The mode that is most affected by the wake field is the one whose mode index μ is such that $-PM - \mu$ is closest to the betatron tune $\nu_\beta = \omega_\beta/\omega_0$ for some integer P, and the leading term in the summation of Eq. (4.114) comes from the term $p = P$. Letting $\nu_\beta = N_\beta + \Delta_\beta$, where N_β is the closest integer to ν_β and Δ_β is between $-\frac{1}{2}$ and $\frac{1}{2}$, we have $\mu = -N_\beta$ (modulo M).[34] Keeping only the leading term in the summation, the growth

[34] For example, if $\nu_\beta = 7.2$ and $M = 3$, we have $N_\beta = 7$, $\Delta_\beta = 0.2$, $P = -3$, $\mu = 2$, and the impedance is to be evaluated at $\omega = 0.2\omega_0$.

rate for this mode is found to be

$$\frac{1}{\tau^{(\mu)}} \approx -\frac{MNr_0c^2}{b^3\gamma\omega_\beta T_0\sqrt{2\pi\sigma\omega_0}}\frac{\text{sgn}(\Delta_\beta)}{\sqrt{|\Delta_\beta|}}, \tag{4.117}$$

which is about M times the growth rate of Eq. (4.34) for a single bunch. It is the *total* beam current that drives the leading mode of transverse resistive-wall instability. This is expected in view of the low frequency nature of the impedance. The mode is damped or antidamped according to whether Δ_β is positive or negative, respectively. Modes with other values of μ are not as affected by the resistive-wall impedance.

When observed in a snapshot at a given time, the bunches executing the above resistive-wall mode have a pattern with $N_\beta \approx \nu_\beta$ oscillations around the accelerator. When observed at a fixed location, however, such as a beam position monitor or a feedback system, the signal has a low frequency $\Delta_\beta\omega_0$ —the same low frequency observed by the resistive-wall impedance. To damp this instability, the bandwidth required by a feedback system is $\Delta f = \Delta_\beta\omega_0/2\pi$, which is typically quite narrow and is easy to provide. In comparison, a feedback system to damp a multibunch instability in general would require a much wider bandwidth, $\Delta f = M\omega_0/2\pi$.

The resistive-wall instability is a more important consideration for large accelerators when there are many bunches. For a given bunch spacing, this shows up as the factor $1/\sqrt{\omega_0}$ in Eq. (4.117), and is a consequence of the impedance sampling at the low frequency $\Delta_\beta\omega_0$. For this reason, the vacuum chamber walls of large circular accelerators are often copper coated.[35]

Exercise 4.12

(a) Consider a beam with 100 equally-spaced bunches, each affecting only the next bunch through the wake function $W_1(-D)$, where D is the bunch spacing. Show that the mode frequencies are given by

$$\Omega^{(\mu)} - \omega_\beta = \frac{Nr_0c^2}{2\gamma C\omega_\beta}W_1(-D)e^{i2\pi(\mu+\nu_\beta)/M},$$

$$\mu = 0, 1, \ldots, 99, \tag{4.118}$$

where $\nu_\beta = \omega_\beta/\omega_0$. Show that 50 modes are damped and 50 are antidamped. What happens if one bunch is removed from the beam so that the "loop" is broken? (Hint: Eigenanalysis does not apply. This accelerator acts like a linac.)

[35]Another reason was mentioned after Eq. (2.194).

(b) Suppose a bunch also weakly affects the second next bunch with $W_1(-2D)$. Show that the mode frequencies are

$$\Omega^{(\mu)} - \omega_\beta = \frac{Nr_0c^2}{2\gamma C\omega_\beta}\left[W_1(-D)e^{i2\pi(\mu+\nu_\beta)/M} + W_1(-2D)e^{i4\pi(\mu+\nu_\beta)/M}\right]. \quad (4.119)$$

What happens if one bunch is removed from the bunch train?[36]

(c) Show that

$$\sum_{\mu=0}^{M-1}\left(\Omega^{(\mu)} - \omega_\beta\right) = 0 \quad (4.120)$$

for both cases (a) and (b). The sum of the growth and damping rates of all modes is zero. The existence of damped modes implies the existence of at least one antidamped mode, and vice versa.

So far we have been considering the transverse multibunch motion. A similar analysis can be applied to the longitudinal case. Again consider M equally spaced bunches, each containing a point charge Ne. The equation of motion for the nth bunch is

$$z_n''(s) + \left(\frac{\omega_{s0}}{c}\right)^2 z_n(s) = \frac{Nr_0\eta}{\gamma C}\sum_k\sum_{m=0}^{M-1} W_0'\left[-kC - \frac{m-n}{M}C + z_n(s) - z_m\left(s - kC - \frac{m-n}{M}C\right)\right], \quad n = 0, 1, 2, \ldots, M-1, \quad (4.121)$$

where ω_{s0} is the unperturbed synchrotron frequency. Let

$$z_n(s) = \tilde{z}_n e^{-i\Omega s/c}, \quad (4.122)$$

and drop the parasitic loss term, as was done following Eq. (4.5). We obtain

$$\left(\Omega^2 - \omega_{s0}^2\right)\tilde{z}_n = -\frac{Nr_0\eta c}{\gamma T_0}\sum_k\sum_{m=0}^{M-1} W_0''\left(-kC - \frac{m-n}{M}C\right) \times\left\{\tilde{z}_n - \tilde{z}_m\exp\left[i\Omega T_0\left(k + \frac{m-n}{M}\right)\right]\right\}. \quad (4.123)$$

[36] F. J. Sacherer, *Proc. Spring Study on Accel. Theory*, Geneva, 1972, p. 175.

The first term in the curly braces is the potential-well term. It can be absorbed into a redefinition of the synchrotron frequency as

$$\omega_s^2 = \omega_{s0}^2 - \frac{Nr_0\eta c}{\gamma T_0}\sum_k \sum_{m=0}^{M-1} W_0''\left(-kC - \frac{M-n}{M}C\right). \tag{4.124}$$

Assuming this incoherent synchrotron frequency shift is small, we may express it in terms of impedance as

$$\Delta\omega_s \approx \frac{MNr_0\eta}{2\gamma T_0^2\omega_s}\sum_{p=-\infty}^{\infty} pM\omega_0 \operatorname{Im} Z_0^{\parallel}(pM\omega_0). \tag{4.125}$$

When $M = 1$, this becomes the first term in Eq. (4.9). Compared with the single-bunch result, the beam intensity is M times larger, but the impedance is sampled M times less frequently.

With a redefinition of synchrotron frequency and written in terms of the impedance, Eq. (4.123) reads

$$(\Omega - \omega_s)\tilde{z}_n = i\frac{Nr_0\eta}{2\gamma T_0^2\omega_s}\sum_{m=0}^{M-1}\tilde{z}_m\sum_p (p\omega_0 + \omega_s)Z_0^{\parallel}(p\omega_0 + \omega_s) \times \exp\left(-i2\pi p\frac{m-n}{M}\right). \tag{4.126}$$

As before, the μth multibunch mode has

$$\tilde{z}_n \propto e^{i2\pi\mu n/M}, \tag{4.127}$$

which, when substituted in Eq. (4.126), gives the mode frequency

$$\Omega^{(\mu)} - \omega_s = i\frac{MNr_0\eta}{2\gamma T_0^2\omega_s}\sum_{p=-\infty}^{\infty}(pM\omega_0 + \mu\omega_0 + \omega_s)Z_0^{\parallel}(pM\omega_0 + \mu\omega_0 + \omega_s). \tag{4.128}$$

This expression is to be compared with Eq. (4.10) and the second term in Eq. (4.9).

Unlike the transverse case, the resistive-wall impedance at low frequencies does not play an important role here. A more instructive application of Eq. (4.128) is for the Robinson instability. Let the fundamental rf cavity mode be sharply peaked around $\omega_R = h\omega_0 + \Delta\omega$, where the harmonic number h is necessarily a multiple of M for a multibunch operation, and $\Delta\omega$ is the amount of frequency detuning. The most unstable mode is the $\mu = 0$ mode,

in which all bunches oscillate in phase. The Robinson growth rate is found from Eq. (4.128) to be a factor of M larger than that predicted by the single-bunch result, Eq. (4.20). The dominant $\mu = 0$ mode for Robinson instability is driven by the total beam current of all bunches. For other modes with $\mu \neq 0$, the Robinson growth rates are small.

4.7 SIMULATION TECHNIQUES

The models introduced in the previous sections of this chapter are limited to a small number of macroparticles. As the number of macroparticles is increased, the analysis rapidly becomes cumbersome. To proceed, one may resort to computers for numerical simulations. With the advent of increasingly powerful computers, numerical simulations have become one of the most effective tools in the study of accelerator beam dynamics in general and the study of collective effects in particular.

By employing a computer, macroparticle models can easily be extended to 10^3 or 10^4 macroparticles, and many more detailed internal modes of the bunch motion can be studied. In addition, simulations also serve the critical function of connecting analyses and experiments.[37] On the one hand, it extends the analysis in the sense that effects not easily studied analytically can be simulated. On the other hand, it modelizes the accelerator in such a way that accelerator operation conditions can be varied at will and free of the obscurities of a real accelerator. We have already mentioned the simulation study of a quadrupole beam breakup effect in a linac in Section 3.3, and the simulation of a two-particle strong head-tail effect in a circular accelerator in Section 4.3. In this section, we will mention a few more examples of simulation studies.[38]

To perform a simulation, one first sets up the problem to be simulated, i.e., one has to know what one intends to learn. This includes determining whether the problem at hand is longitudinal or transverse or both, and whether the wake field is short-ranged or long-ranged. One chooses a short range wake field (for a broad-band impedance) to study single-bunch effects, and long range one (for a sharply peaked impedance) to study multibunch or multiturn effects. One may also choose to emphasize the interplay between two separate effects, which is where analyses typically have the most difficulties. In a simulation, one usually stays in the time domain, which means it is more convenient to use the wake functions than the impedances. The impedance is often considered to be lumped at some fixed location(s) in the accelerator.

[37]As one might say, simulation is the geometric mean between analysis and experiment.

[38]Examples are chosen for illustration only. The reader is encouraged to explore these topics in the literature. See for example, R. H. Siemann, Nucl. Instr. Meth. **203**, 57 (1982); D. Brandt and B. Zotter, *Proc. 12th Int. Conf. High Energy Accel.*, Fermilab, 1983, p. 309.

Consider a circular accelerator and a single-bunch beam modeled as M macroparticles. Let the jth macroparticle have charge $N_j e$, where $\sum_{j=1}^{M} N_j = N$ is the total number of particles in the bunch. The beam bunch passes by a lumped impedance, which we assume is where the rf cavity sits, once per revolution. Consider a particular revolution. Let z_j be the longitudinal position of the jth macroparticle ($z > 0$ is the bunch head), so that it arrives at the impedance at time $-z_j/c$ relative to the synchronous particle, which is considered to be located at the bunch center and unperturbed by the wake fields. Let δ_j, y_j, and y_j' be the relative energy error, the transverse displacement, and the transverse slope of the jth macroparticle as it passes by the impedance. Let the transverse and longitudinal wake functions due to the impedance be $W_1(z)$ and $W_0'(z)$.[39]

We are now in a position to write down the transverse and longitudinal wake forces experienced by a test charge e in the jth macroparticle. First consider the case when the wakes are short-ranged. A test charge in the leading macroparticle (the one with the largest value of z_j in the particular passage under consideration) will experience

$$\int ds\, F_{\parallel} = -\tfrac{1}{2} N_j e^2 W_0'(0^-) \quad \text{and} \quad \int ds\, F_{\perp} = 0. \tag{4.129}$$

For a test charge in a later macroparticle, say the jth, we have

$$\begin{aligned} \left(\int ds\, F_{\parallel}\right)_j &= -\tfrac{1}{2} N_j e^2 W_0'(0^-) \\ &\quad - \sum_{k \neq j} N_k e^2 \left[W_0'(z_j - z_k) + y_k y_j W_1'(z_j - z_k) \right], \\ \left(\int ds\, F_{\perp}\right)_j &= -\sum_{k \neq j} N_k e^2 y_k W_1(z_j - z_k), \end{aligned} \tag{4.130}$$

where the summation over $k \neq j$ is over the macroparticles, except that macroparticles behind the jth do not contribute to the sums, because $W_0(z)$ and $W_1(z)$ vanish if $z > 0$. The quantities $\int ds\, F_{\parallel}$ and $\int ds\, F_{\perp}$ couple the dynamic variables of a macroparticle to those of the other macroparticles. The W_1' term in Eq. (4.130) gives the longitudinal effect of the $m = 1$ wake field.

In case the wakes are long-ranged so that they are longer than the accelerator circumference C, we have to take into account contributions from

[39] Here we consider simultaneously the $m = 0$ and the $m = 1$ wake fields, but ignore the $m = 2$ wake fields. To include the $m = 2$ wake effects would be more involved; in particular, the dynamic variables of the macroparticles will have to include, in addition to z_j, δ_j, y_j, and y_j', also the other transverse coordinate x_j, its slope x_j', and the normal and skew second moments Q_{nj} and Q_{sj}.

residual wake fields from previous revolutions. Equation (4.130) then acquires the following additional terms:

$$\left(\int ds\, F_{\parallel}\right)_j = -\sum_{m=1}^{\infty}\sum_{k=1}^{M} N_k e^2 \left[W_0'\left(z_j - z_k^{(m)} - mC\right) + y_k^{(m)} y_j W_1'\left(z_j - z_k^{(m)} - mC\right)\right], \quad (4.131)$$

$$\left(\int ds\, F_{\perp}\right)_j = -\sum_{m=1}^{\infty}\sum_{k=1}^{M} N_k e^2 y_k^{(m)} W_1\left(z_j - z_k^{(m)} - mC\right),$$

where $z_k^{(m)}$ and $y_k^{(m)}$ are the coordinates of the kth macroparticle m revolutions before.

The changes of the dynamic variables of the jth macroparticle as the bunch passes by the impedance can be written in a matrix form,

$$\begin{bmatrix} \Delta z_j \\ \Delta \delta_j \\ \Delta y_j \\ \Delta y_j' \end{bmatrix} = \frac{1}{E} \begin{bmatrix} 0 \\ \left(\int ds\, F_{\parallel}\right)_j - eV_{\mathrm{rf}} \sin \dfrac{\omega_{\mathrm{rf}} z_j}{c} \\ 0 \\ \left(\int ds\, F_{\perp}\right)_j \end{bmatrix}. \quad (4.132)$$

An extra term proportional to the rf voltage V_{rf} has been added to δ_j because we have assumed the impedance is located at the rf cavity. If nonlinearities of the rf focusing are not important in the study, one may replace $\sin(\omega_{\mathrm{rf}} z_j/c)$ by $\omega_{\mathrm{rf}} z_j/c$.

The transformation of the dynamic variables between impedances is given by the unperturbed betatron and synchrotron motions prescribed by the accelerator design.[40] For example, if the betatron motion is that of a simple harmonic motion, we have

$$\begin{bmatrix} z_j \\ \delta_j \\ y_j \\ y_j' \end{bmatrix}_s = \begin{bmatrix} 1 & -\eta & 0 & 0 \\ 0 & 1 & 0 & 0 \\ 0 & 0 & \cos \dfrac{\omega_\beta s}{c} & \dfrac{c}{\omega_\beta} \sin \dfrac{\omega_\beta s}{c} \\ 0 & 0 & -\dfrac{\omega_\beta}{c} \sin \dfrac{\omega_\beta s}{c} & \cos \dfrac{\omega_\beta s}{c} \end{bmatrix} \begin{bmatrix} z_j \\ \delta_j \\ y_j \\ y_j' \end{bmatrix}_0. \quad (4.133)$$

If the only impedance is located at the rf cavity, one has $s = C$.

The simulation procedure is then to apply Eqs. (4.132–4.133) alternately between the impedance and the accelerator section. The beam bunch is

[40] E. D. Courant and H. S. Snyder, Ann. Phys. **3**, 1 (1958).

launched with a certain set of initial values of the dynamic variables of all of its macroparticles, and the evolution of these variables is observed as the simulation proceeds.

Calculation of the multiturn wake forces using Eq. (4.131) involves double summations—one over the macroparticles, the other over the previous revolutions—which consume much computer time. For resonator impedances, however, this can be avoided by noting that the wake function can be written as a phasor[41] according to

$$W_0'(z) \equiv \operatorname{Re} \tilde{W}_0'(z), \qquad z < 0. \tag{4.134}$$

It follows from Eq. (2.84) that $\tilde{W}_0'$ satisfies the phasor condition

$$\tilde{W}_0'(z + D) = \tilde{W}_0'(z) e^{(i\bar{\omega}+\alpha)D/c}, \qquad D < 0, \tag{4.135}$$

where the parameters α and $\bar{\omega}$ were defined in Eq. (2.84). The same expressions hold for the $m = 1$ wake functions W_1 and W_1', provided the parameters α and $\bar{\omega}$ are taken from the $m = 1$ impedance.

The double summations in Eq. (4.131) can now be simplified. For example, one of the terms on the right hand side can be written as

$$\begin{aligned} -\sum_{m=1}^{\infty}\sum_{k=1}^{M} N_k e^2 \tilde{W}_0'\left(z_j - z_k^{(m)} - mC\right) &= -\sum_{k=1}^{M} N_k e^2 \tilde{W}_0'\left(z_j - z_k^{(1)} - C\right) \\ &\quad -\sum_{m=2}^{\infty}\sum_{k=1}^{M} N_k e^2 \tilde{W}_0'\left(z_j - z_k^{(m)} - mC\right). \end{aligned} \tag{4.136}$$

The second term on the right hand side of Eq. (4.136) can be written as

$$\begin{aligned} -\sum_{m=1}^{\infty}\sum_{k=1}^{M} N_k e^2 \tilde{W}_0'\left[z_j - z_k^{(m+1)} - (m+1)C\right] \\ = -\sum_{m=1}^{\infty}\sum_{k=1}^{M} N_k e^2 \tilde{W}_0'\left(z_j^{(1)} - z_k^{(m+1)} - mC\right) e^{-(i\bar{\omega}+\alpha)(C+z_j^{(1)}-z_j)}. \end{aligned} \tag{4.137}$$

The term in front of the phase factor on the right hand side of Eq. (4.137) is the same quantity already calculated for the jth macroparticle in the previous revolution. If this information has been stored in the computer, the double summation reduces to a single summation over the macroparticles. A similar reduction occurs in the other two double summations in Eq. (4.131). The first term in Eq. (4.136) gives the wake field excited by the beam in the last revolution. The second term gives the ringing wake fields accumulated over all previous revolutions.

[41] Perry B. Wilson, *AIP Proc.* **87**, *Phys. High Energy Part. Accel.*, Fermilab, 1981, p. 450.

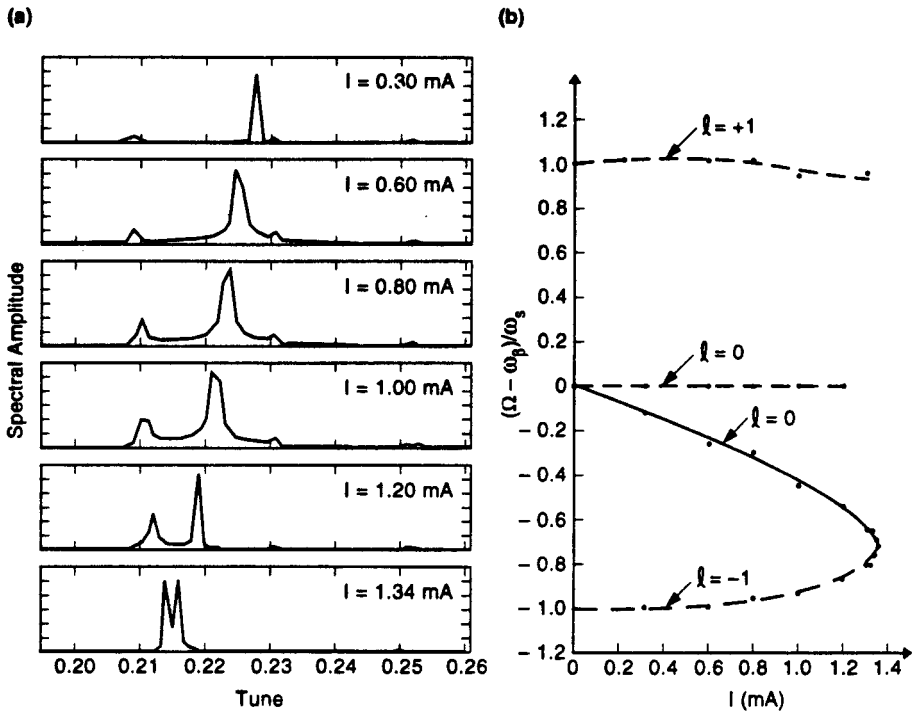

Figure 4.16. Simulation of the strong head-tail instability for the PEP storage ring. (a) Spectrum of the beam center of charge showing the collective modes for several beam intensities. (b) Mode frequencies $(\Omega - \omega_\beta)/\omega_s$ versus the average beam current $I = Ne/T_0$. (Courtesy Steve Myers, 1992.)

Figure 4.16 is a simulation result performed for the PEP storage ring at 4.5 GeV.[42] What is being studied is the strong head-tail instability. The impedance is assumed to come from the rf cavities. Figure 4.16(a) shows the Fourier spectrum of the beam center of charge for various beam intensities. We observe four mode frequency peaks of varying strengths; one corresponds to mode index $l = -1$, one to $l = 1$, and two to $l = 0$.[43] The most prominent feature is the gradual convergence of the frequencies of the $l = -1$ and one of the $l = 0$ modes as the beam intensity is increased. When they merge, at a beam current of $I = 1.4$ mA, the beam becomes unstable. Figure 4.16(b) is a plot of the mode frequencies versus I. The behavior is in good agreement with the two-particle model for the lowest modes.

Another simulation for PEP of the head-tail instability is shown in Figure 4.17.[44] When the chromaticity $\xi < 0$, one observes from Figure 4.17(a) that

[42]Stephen Myers, *Proc. IEEE Part. Accel. Conf.*, Washington, 1987, p. 503.

[43]Discussion of these various modes, beyond those of the two-particle model, is the subject of Sections 6.6 and 6.7.

[44]R. H. Siemann, Nucl. Instr. Meth. **221**, 293 (1984); R. H. Siemann, *AIP Proc.* **127**, Phys. High Energy Part. Accel., BNL/SUNY, 1983, p. 368.

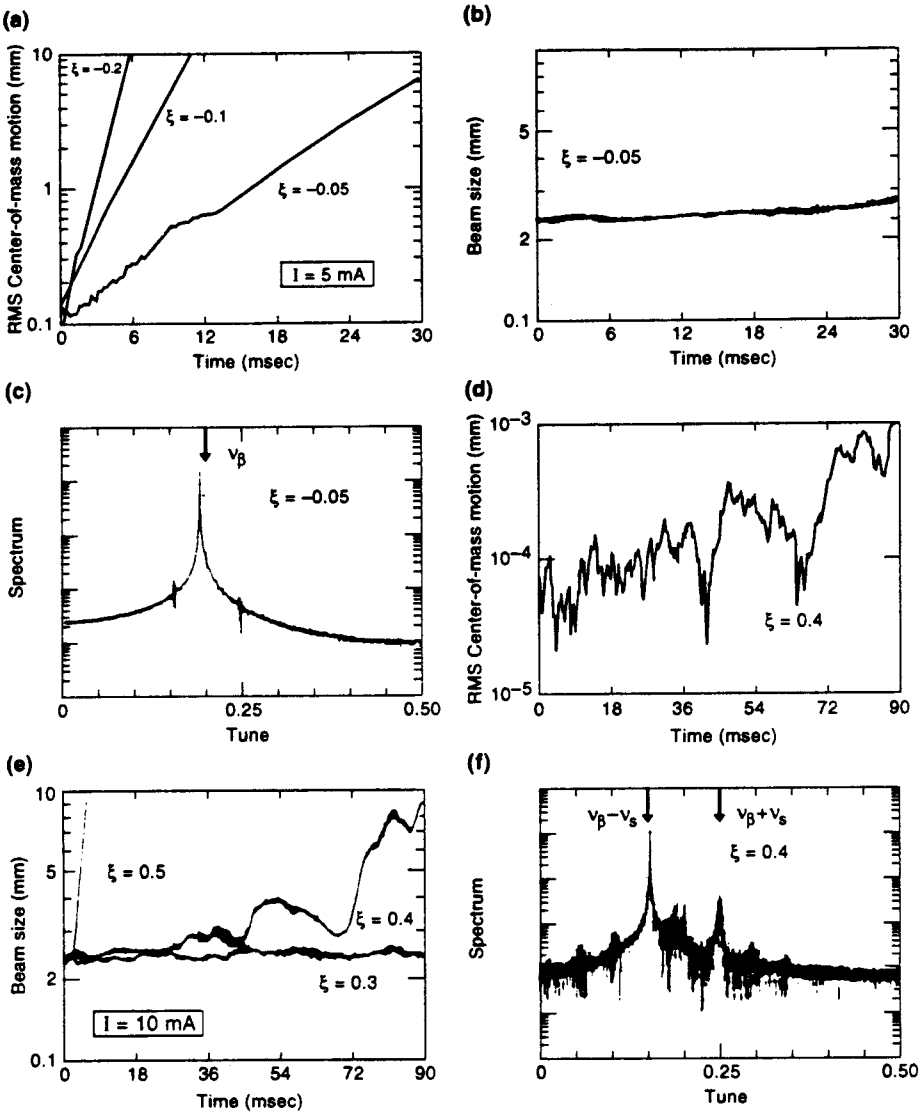

Figure 4.17. Simulation of the head-tail instability for the PEP storage ring. (a) The amplitude of the beam center-of-charge motion grows with the beam storage time for three values of $\xi < 0$ and a fixed beam current $I = 5$ mA. (b) The beam size stays basically constant when $\xi < 0$. (c) Spectrum of the beam center-of-charge motion for a negative ξ. (d), (e), and (f) are the same as (a), (b), and (c), but for $\xi > 0$. Arrows in (c) and (f) indicate the unperturbed betatron tune $\nu_\beta = \omega_\beta / \omega_0$ and its synchrotron sidebands $\nu_\beta \pm \nu_s$. (Courtesy Robert Siemann, 1992.)

the amplitude of the beam center-of-charge motion (reflecting the + mode) becomes unstable and grows exponentially with a growth rate more or less proportional to ξ. Figure 4.17(b) shows that when $\xi < 0$, the rms beam size (reflecting the − mode) stays basically constant. The center-of-charge motion is Fourier analyzed to yield the spectrum shown in Figure 4.17(c). When $\xi > 0$, the behavior is reversed as shown in Figures 4.17(d) and (e), i.e., the beam center of charge stays basically constant, whereas the beam size grows exponentially. Since PEP is operated above transition, this behavior is consistent with the results from Eq. (4.99) of the two-particle model. The beam spectra in Figures 4.17(c) and (f) are also consistent with this picture: when $\xi < 0$, the beam is mainly executing a center-of-charge motion near the betatron frequency; when $\xi > 0$, the beam motion is mainly in the $l \neq 0$ modes, particularly the $l = \pm 1$ modes with mode frequencies near $\omega_\beta \pm \omega_s$.

The flexibility of simulation studies allows them to include effects in addition to the wake field effects to be studied simultaneously. For example, one may include radiation damping and quantum excitation, which play a role in circular electron accelerators. The interplay between collective phenomena and nonlinearities in single-particle motion can be simulated by including nonlinear terms in the transformation (4.133). Landau damping effects (see Chapter 5) can be simulated by including spreads in the unperturbed synchrotron or betatron frequencies of the macroparticles. Inclusions of synchro-betatron coupling, more realistic wake functions, localized impedances, and feedback systems are straightforward in a simulation.

The choice of the number of macroparticles, M, depends on the problem at hand. In practice, one varies M until the result stabilizes, and makes the choice after judging against the computer time consumed. Two considerations affect the choice of M: one is dynamics, and the other is statistics. The dynamical consideration is that the number of macroparticles must be larger (if possible, much larger) than the highest order of the modes of interest. A simulation of the longitudinal bunch lengthening phenomenon (see Section 6.5), for example, tends to require a large M because higher modes are involved in the dynamics. The statistical consideration is more pronounced in the studies of longitudinal instabilities. It comes from the fact that the wake function is discontinuous at $z = 0$. One close encounter between two macroparticles can lead to very different subsequent results, depending on which particle happens to be slightly ahead. One way to improve the statistics is to increase M. Another, adopted in obtaining Figure 4.17, is to write the instantaneous beam distribution as a superposition of orthogonal polynomials, the expansion coefficients of which are fitted every time the beam passes by the impedance. The expansion is truncated at some order, and the truncation order then plays a role equivalent to the number of macroparticles, except that the noise problem is much eased.